

NASA Contractor Report 182293
DOT/FAA/CD-89/13

Droplet Sizing Instrumentation Used for Icing Research: Operation, Calibration, and Accuracy

Edward A. Hovenac
Sverdrup Technology, Inc.
NASA Lewis Research Center Group
Cleveland, Ohio

August 1989

Prepared for
Lewis Research Center
Under Contract NAS3-25266

and

Department of Transportation
Federal Aviation Administration



U.S. Department of Transportation
Federal Aviation Administration

(NASA-CR-182293) DROPLET SIZING
INSTRUMENTATION USED FOR ICING RESEARCH:
OPERATION, CALIBRATION, AND ACCURACY Final
Report (Sverdrup Technology) 55 p CSCL 14B

N90-11999

Unclas
65/35 0239280

NOTICE

This document is disseminated under the sponsorship of the U. S. Department of Transportation in the interest of information exchange. The United States Government assumes no liability for the contents or use thereof.

The United States Government does not endorse products or manufacturers. Trade or manufacturers' names appear herein solely because they are considered essential to the objective of this report.

TABLE OF CONTENTS

	Page
EXECUTIVE SUMMARY	iv
1. INTRODUCTION	1
2. OPERATION OF THE FORWARD SCATTERING SPECTROMETER PROBE	1
2.1 Theory of Operation	1
2.2 Operating Procedures in an Icing Environment	3
2.3 Measurement of Optical and Electronic Parameters	5
3. CALIBRATION OF THE FSSP	11
3.1 Glass Beads	12
3.2 The Monodisperse Droplet Generator	14
3.3 The Rotating Pinhole -- A New Calibration Device	16
3.4 Comparison of the Various Calibration Techniques	18
4. ACCURACY OF THE FSSP	18
4.1 Number Density Errors	21
4.2 Velocity Errors	25
4.3 Calibration Errors	27
4.4 Laser Beam Illumination Errors	32
4.5 Size-Velocity Correlation Errors	35
4.6 Overall Accuracy of the FSSP	38
5. OPERATION OF THE OPTICAL ARRAY PROBE	39
5.1 Theory of Operation	39
5.2 Measurement of Optical Characteristics	39
6. CALIBRATION OF THE OAP	43
7. ACCURACY OF THE OAP	45
8. CONCLUSIONS	45
9. REFERENCES	46

LIST OF FIGURES

Figure	Page
2.1	Ice Buildup on the FSSP in NASA's Icing Research Tunnel 4
2.2	Voltages From the Signal and Annulus Detectors 7
2.3	Calibration Curves for the FSSP for Different Optical Collection Angles 7
2.4	Diffraction Pattern From a 25 Micrometer Pinhole 8
2.5	Using a Diffraction Pattern to Measure Collection Angles in the FSSP 8
2.6	Measurement of the Delay Times in the FSSP 10
3.1	Transfer Function Relating Glass Bead Diameter to Water Droplet Diameter in the FSSP 10
3.2	Comparison of Theoretical Calibration Curves in the FSSP 13
3.3	Signal Generated by Droplets Crossing the Probe Volume in the FSSP 13
3.4	The Rotating Pinhole Calibrator 15
3.5	Transfer Function Relating Pinhole Diameter to Water Droplet Diameter in the FSSP 17
3.6	The FSSP Response to Several Common Size Pinholes 17
3.7	Using the Rotating Pinhole to Align the FSSP 19
3.8	Calibration of the FSSP Using Glass Beads 20
3.9	Calibration of the FSSP Using Rotating Pinholes 20
3.10	Distribution From a Monodisperse Droplet Generator 20
4.1	Comparison of Droplet Size Distributions Measured in the NASA Icing Research Tunnel 22

Figure		Page
4.2	Coincidence Errors Brought on By High Number Density	24
4.3	FSSP Response to Short Duration Optical Pulses	26
4.4	Small Particle Velocity Errors in the FSSP	26
4.5	Calibration Accuracy of the NASA Lewis Extended Range FSSP	28
4.6	Comparisons Between the FSSP and the Phase Doppler Particle Analyzer.	30
4.7	Theoretical Calibration Curve Compared With the Instrument Calibration Curve	31
4.8	Calibration Error Simulation	33
4.9	Intensity Cross Section in the FSSP Laser Beam	33
4.10	Intensity Fluctuations Depend on Particle Diameter	34
4.11	Broadening of the Size Spectrum Caused by Uneven Laser Beam Illumination	36
4.12	Mathematical Model Describing Spectral Broadening in the FSSP	36
4.13	Spectral Broadening Simulation	37
4.14	Simulation Showing the Effects of a Size-Velocity Correlation in the FSSP	37
4.15	The Overall Accuracy of the FSSP	40
5.1	Measured Diameter of Reticle Disks as a Function of Depth of Field in the OAP	42
5.2	Counting Probability in the OAP	42
6.1	Calibration Curve for the OAP Using the Rotating Reticle	44

EXECUTIVE SUMMARY

The Forward Scattering Spectrometer Probe (FSSP) and the Optical Array Probe (OAP) are particle sizing instruments that can be used to measure droplet diameters in icing clouds. The operation, calibration, and accuracy of these instruments are examined.

Operation of the FSSP and the OAP in an icing environment may cause them to become clogged with ice even with the onboard heaters in operation. Also, their optical components may become contaminated with water droplets and cause the instrument to make sizing errors. Purge air can help to alleviate this problem.

Measurement of certain optical and electronic parameters is recommended to improve the confidence in the data obtained with the instruments. Methods for making these measurements are given in detail. These include measurements of the beam diameter, depth of field, optical collection angles, and the electronic dead times. Most notable of these is an innovative method to measure the optical collection angles using the diffraction pattern from a pinhole.

Calibration of the FSSP is described by using three methods: glass beads, a droplet generator, and a rotating pinhole device. Both the theoretical and practical advantages and disadvantages of each method are explored. Methods for improving the performance of the droplet generator are presented. The rotating pinhole device is a new calibration method developed at NASA Lewis and has the potential for being a new standard for calibration of the FSSP.

Accuracy of the FSSP is estimated by testing individual instrument components, by using computer simulations, and by comparing with other droplet sizing instruments. The magnitude of sizing errors in the FSSP is found to be the result of many factors including number density, velocity, size/velocity correlation, and calibration errors.

The operation and calibration of the OAP are also examined. Most notable is the development of a calibration reticle for the OAP.

1. INTRODUCTION

The NASA Lewis Research Center is conducting research in aircraft icing, supported in part by the FAA. One area of interest is the characterization of icing clouds. Information from the study of icing clouds enables researchers to more accurately model ice formation on aircraft, design de-icing systems, and improve the safety of winter flights.

Icing clouds may be studied in wind tunnels and from heavily instrumented research aircraft. The diameter of the water droplets in icing clouds is one parameter that is of interest. Measurement of droplet size distributions in icing clouds may be performed with the Forward Scattering Spectrometer Probe (FSSP) and the Optical Array Probe (OAP), both are manufactured by Particle Measuring Systems, Inc., of Boulder, Colorado. This report addresses the operation, calibration, and accuracy of these two instruments.

2. OPERATION OF THE FORWARD SCATTERING SPECTROMETER PROBE

2.1 Theory of Operation

The Forward Scattering Spectrometer Probe is an optical particle sizing instrument used for the measurement of water droplet diameters in natural and artificial clouds. Details about the theory of operation of the FSSP are described in the FSSP manual (ref. 1) and several other papers (refs. 2 and 3). This section discusses only the features about the FSSP that relate to the analysis in future sections.

The FSSP measures the diameter of a droplet by measuring the intensity of light scattered by that droplet as it crosses a focused laser beam. Different regions of the laser beam have different intensities. This could cause sizing errors since the intensity of light a droplet scatters is proportional to the light incident upon it. One method of minimizing this error is to only make measurements in the region of the beam where the light intensity is nearly constant. This region is called the probe volume.

A well defined probe volume in the instrument is critical to an accurate measurement. All droplets crossing the laser beam within the probe volume must be measured and all droplets crossing the laser beam outside of the probe volume must be rejected. The physical shape of the probe volume is cylindrical and can be described in terms of its radial and axial components.

The radial dimension of the probe volume is defined by the transit time of the droplets through the volume. It is assumed that all the droplets to be measured are moving at the same velocity. Some droplets will traverse a chord of the beam that is close to the (radial) edge of the beam. These droplets will be in the beam for a shorter period of time and will have a short transit time. The transit time of each droplet that goes through the probe volume is measured and combined with the average transit time of all the previous droplets that went through the probe volume. If the droplet has a transit time that is shorter than the average, then it is outside of the probe volume and it is rejected.

The actual measurement of the transit time must be made to minimize the effects of droplet size. For example, if the start of the transit time is determined by the leading edge of the droplet and the end of the transit time

by the trailing edge, then large droplets would have longer transit times than small ones. The probe volume reject criterion would not only be a function of the droplet's radial trajectory (as it should be) but also a function of droplet's diameter. This would bias the measurement toward larger droplets. To avoid this problem, the transit time is measured from the time the center of the droplet enters the laser beam to the time that the center leaves the beam. This is done by analyzing the scattered light as the droplet passes through the laser beam. When the scattering is at 50 percent of its maximum value, then it is assumed the center of the droplet is either entering or leaving the laser beam. A delay circuit is needed to determine this 50-percent level. The signal is divided into two parts: a delayed part and an undelayed part. First the peak voltage of the undelayed signal is determined. Fifty percent of this peak voltage is stored for comparison with the delayed signal. When the delayed signal arrives at a comparator, its voltage level is compared with the stored 50-percent voltage level. As soon as the delayed signal exceeds the 50-percent level, the transit time clock is turned on. When the delayed signal drops back down below the 50-percent level, because the droplet left the probe volume, the clock is turned off. In this way the transit time is not a function of the droplet's diameter.

The axial component of the probe volume (or the depth of field) extends to either side of the waist of the laser beam. The depth of field is determined by assessing the divergence of the light coming into a photodetector. The optical system is arranged so that when a droplet (or any object that scatters light) is at the waist of the laser beam, the scattered light will be focused to a point on the photodetector. If the object scattering light is away from the waist, then the light impinging on the detector will diverge and blur into a disk rather than a point. If the disk of light is too large then the water droplet is too far from the waist and is outside of the probe volume.

To assess the divergence of light at the photodetector, a beam splitter directs a portion of the scattered light to another photodetector with a circular mask or dump spot in front of it. If the blur spot diverges enough so that it is larger than the mask, then some of the light will spill over the edge of the mask and into the photodetector. The signal from this detector is amplified and compared with the signal coming from the unmasked photodetector. If the voltage coming from the masked detector (also called the annulus detector) is greater than the voltage coming from the unmasked detector (also called the signal detector) then the droplet is outside of the probe volume.

The signal detector is the component responsible for making the size determination. As the droplet crosses the laser beam, the light scattered by the droplet is focused onto the signal detector. The signal detector produces a voltage pulse proportional to the intensity of light incident on it. The peak voltage is proportional to the intensity when the droplet is totally within the laser beam. The diameter of the droplet can be determined from the peak voltage by using a calibration curve that relates voltage to droplet diameter.

2.2 Operating Procedures in an Icing Environment

The operating manual for the FSSP covers most of the standard procedures for aligning and operating the FSSP. However, operating in an icing environment presents some added problems that need to be addressed.

The most notable problem is the buildup of ice on the instrument. Although the photograph in figure 2.1 is an extreme case, ice buildup on the FSSP is nevertheless the condition that causes the most delays when performing icing wind tunnel tests. For ice removal, the tunnel must first be brought down to idle, the ice removed from the instrument, and then the tunnel must be brought back up to velocity and temperature.

The reason the ice needs to be removed from the probe is that it tends to choke off the flow through the sample volume of the FSSP. This can occur at three critical positions on the FSSP.

The first position is at the front of the flow straightening tube. This occurs during conditions of high liquid water content and when the temperature is so cold that the FSSP heater cannot keep the ice melted on the leading edge of the flow straightening tube. The ice does not build up uniformly in this region as one would expect, but rather starts on the transmitter side of the tube and grows until the flow is choked off. There are two FSSPs at NASA Lewis and both behave in this same peculiar way. This is probably caused by the design of the heater in the flow straightening tube.

To help melt the ice on the front of the flow straightening tube during particularly cold tests, the voltage on the heaters is sometimes raised several volts above the recommended level. This keeps the front of the tube clean but causes another icing problem. Because only the front half of the flow straightening tube is heated, there is water runoff from the front section to the back. When the water reaches the back section that is unheated, it freezes. Again the ice builds up until the flow is choked off. This can also be seen in figure 2.1.

The third place where ice causes problems is at the laser exit inside of the flow straightening tube. There is a small protrusion at this location that keeps water droplets from entering the optical system. This protrusion can build up enough ice to distort the flow through the probe volume or even obscure the laser beam. What makes this problem hard to detect is that it is difficult to see inside the flow straightening tube during a tunnel test. Where the other icing problems are obvious, this one is not.

One problem that occurs regularly during runs in the NASA Lewis Icing Research Tunnel (IRT) is the accumulation of water on the optical components of the FSSP. Almost always the components that get wet are on the receiver side of the optical train including the 90° prism, the focusing lens package, and even as far back as the beam splitter. The water on the 90° prism is probably a result of water splashing off of the optical ports. Contamination of the other components is likely caused by condensation. This problem necessitates regular calibration checks during icing tunnel runs to insure the optical system has not become too badly contaminated. Once contamination occurs, the only solution is to remove the instrument and dry off the components.

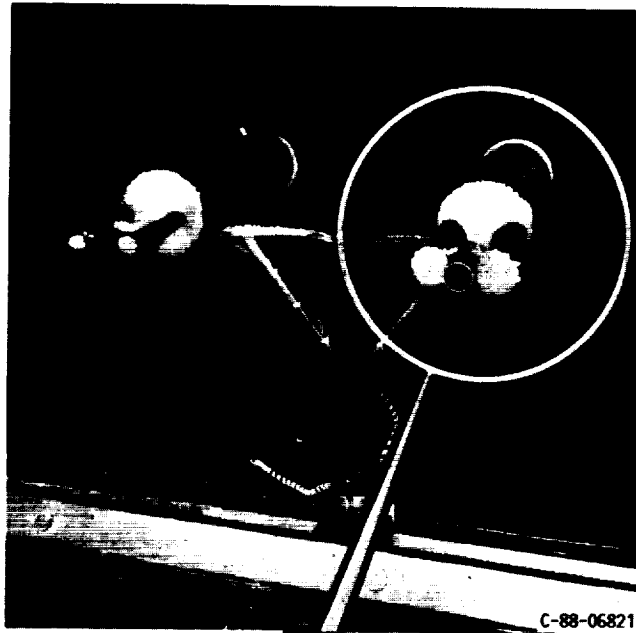


FIGURE 2.1. - ICE BUILDUP ON THE FSSP IN NASA'S ICING RESEARCH TUNNEL.

ORIGINAL PAGE
BLACK AND WHITE PHOTOGRAPH

One way to reduce the optical contamination problem is to run purge air through the FSSP between icing runs. This will help evaporate any droplets that accumulated during the previous icing run. Using purge air while data is being taken is not recommended because the velocity of the purge air exiting the optical ports can alter the trajectory of the droplets in the probe volume.

When setting up the FSSP to run purge air, the user must be certain an adequate volume of air can exit both probe arms through the optical ports. In the FSSPs at NASA Lewis, the probe arm with the laser in it has a much larger exit area for the purge air than the receiver side. To compensate, the points of greatest constriction in the receiver arm were located and enlarged. This turned out to be at the box containing the photodetector module (a hole was drilled in the box) and the mount containing the beam splitter (a slot was machined in the mount). This allowed purge air to be injected into the rear of the FSSP and exit equally through both probe arms.

2.3 Measurement of Optical and Electronic Parameters

Certain optical and electronic parameters of the FSSP need to be determined to improve confidence in the measurements made by the instrument. These parameters may not be included in the operation manual, or it may be suspected that certain parameters have changed over a period of time, or the user may want to verify the values given in the manual. Included below are several procedures for measuring these parameters and the results of these measurements for one FSSP used at NASA Lewis.

Before making any measurements, a few tools are necessary. These include an oscilloscope or at least a voltmeter, and a micropositioning stage. Also, if detailed lab tests are to be conducted on the FSSP the flow straightening tube should be removed to make access to the laser beam easier.

The flow straightening tube can be removed by unscrewing the four screws on either end of the tube. The heater wires in the flow straightening tube will need to be unplugged from inside the probe arm. Since the friction between the probe arms and the flow straightening tube will not allow the tube to slide off, one of the probe arms will also need to be removed. The receiver arm is easily removed. First remove the box containing the photodetector module (four screws). This will expose the four screws holding the probe arm in place. Remove these screws and pull the arm forward. This will release the tension on the flow straightening tube and allow it to be removed. Next, replace the probe arm and photodetector box, and realign the instrument by following the manufacturer's recommended procedure.

With the flow straightening tube removed, access to the laser beam will be much easier, making measurement of the optical parameters less tedious. Two such parameters are the laser beam diameter and the depth of field. Since they define the probe volume, these parameters must be precisely determined to permit accurate number density measurements with the FSSP.

The diameter of the laser beam is given in the manual. Checking it can be very subjective since the laser beam does not have a sharp cutoff and the beam does not have a Gaussian intensity profile. The easiest method is to take one strand of a nylon fiber (less than 25 μm in diameter) and attach it to a paper clip by using rubber cement. Attach the paper clip to a micropositioning table

and move the fiber into the beam. Check the voltage of the signal and annulus detectors at the stage after the range amplifiers (pin #10 on IC HA2405). If the voltage coming from the annulus detector is greater than the voltage from the signal detector, then the fiber is not in the center of the depth of field. Reposition the fiber axially in the laser beam until the signal voltage is greater than the annulus voltage. Next, move the fiber radially through the beam noting the two positions where the voltage is approximately half of the maximum voltage. The distance between these two points is the beam diameter.

The easiest way to measure the depth of field is to move a piece of translucent tape axially along the laser beam. The voltages for the signal and annulus detectors can be monitored at the same place the voltages for the beam diameter were monitored. The place where the signal voltage becomes greater than the annulus voltage is the beginning of the depth of field. As the tape is moved farther down the beam in the axial direction, the annulus voltage will increase to a value greater than the signal voltage. This is the end of the depth of field. A plot showing the signal and annulus voltages as a function of position is given in figure 2.2. The depth of field is the distance between the cross over points.

The depth of field is one value that can change from the manufacturer's specifications. A test was performed in which the FSSP was intentionally misaligned then realigned, then the depth of field was measured. This procedure was repeated eight times to see the effect of subtle differences in alignment on the depth of field. For eight measurements of the depth of field, a spread in the measurement of ± 12 percent (the standard deviation was ± 8 percent) was observed. This exercise demonstrates that the depth of field is not an instrument constant and should be measured prior to any tests where number density or liquid water content are to be measured.

Another optical parameter that needs to be known is the optical collection angles. These angles can change the calibration curve for the FSSP. Typical values of the collection angles are 4° for the inner angle and 14° for the outer angle. These values determine how much scattered light impinges on the detectors in the FSSP. Figure 2.3 shows the effect (on the theoretical calibration curve) of changing the inner angle and the outer angle. The accuracy of the calibration curve is dependent on the measured accuracy of these angles. Measuring the collection angles by using a ruler or a micrometer is very difficult because of the space restrictions in the probe arms. An alternative method is suggested below.

A pinhole of a known diameter can be used to measure the collection angles. The pinhole, when placed in the center of the depth of field will create a diffraction pattern at the detector plane of the FSSP. The diffraction pattern looks like a region of light and dark rings. The angular position of these rings is a function of the pinhole diameter and the wavelength of the laser beam. Both are known. Thus the diffraction rings act as a scale to measure the collection angles of the instrument.

To make the measurement, a 25- μm pinhole is a good size to use. It will create a diffraction pattern with enough rings to make an accurate measurement and not so many that they are spaced too close together to count. Place the pinhole in the center of the laser beam and the center of the depth of field.

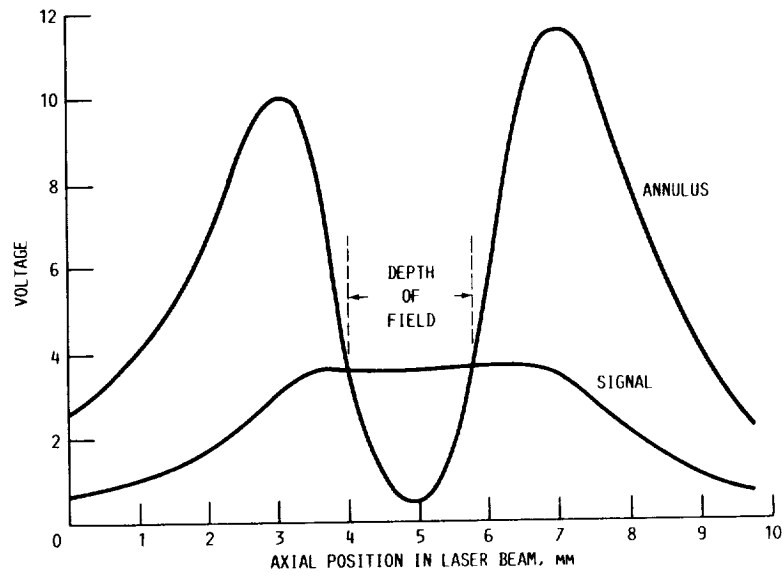


FIGURE 2.2. - VOLTAGES FROM THE SIGNAL AND ANNULUS DETECTORS DEFINE THE DEPTH OF FIELD.

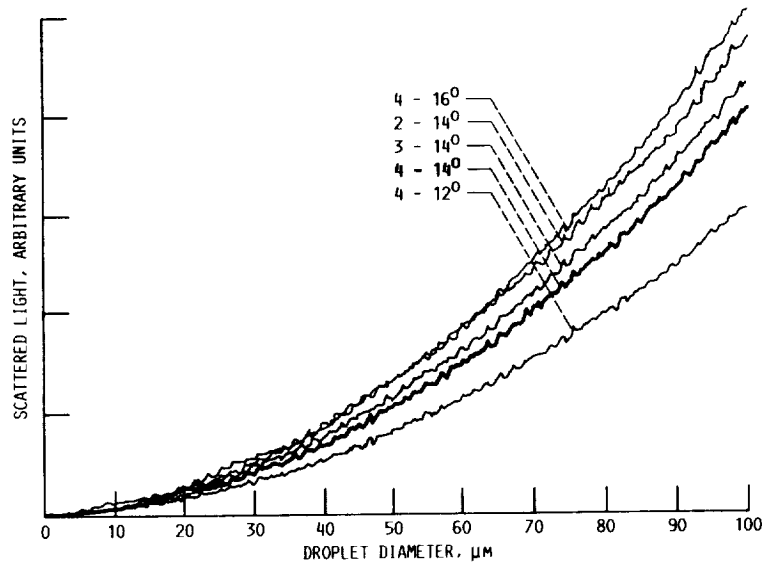


FIGURE 2.3. - CALIBRATION CURVES FOR THE FSSP FOR DIFFERENT OPTICAL COLLECTION ANGLES.

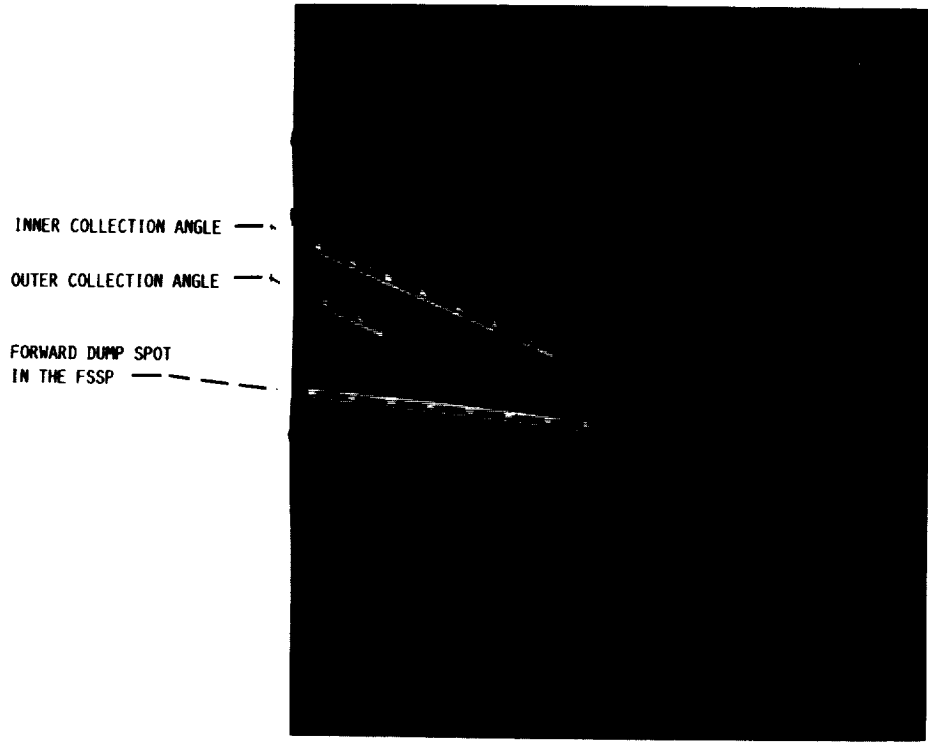


FIGURE 2.4. - DIFFRACTION PATTERN FROM A 25 μm PINHOLE.

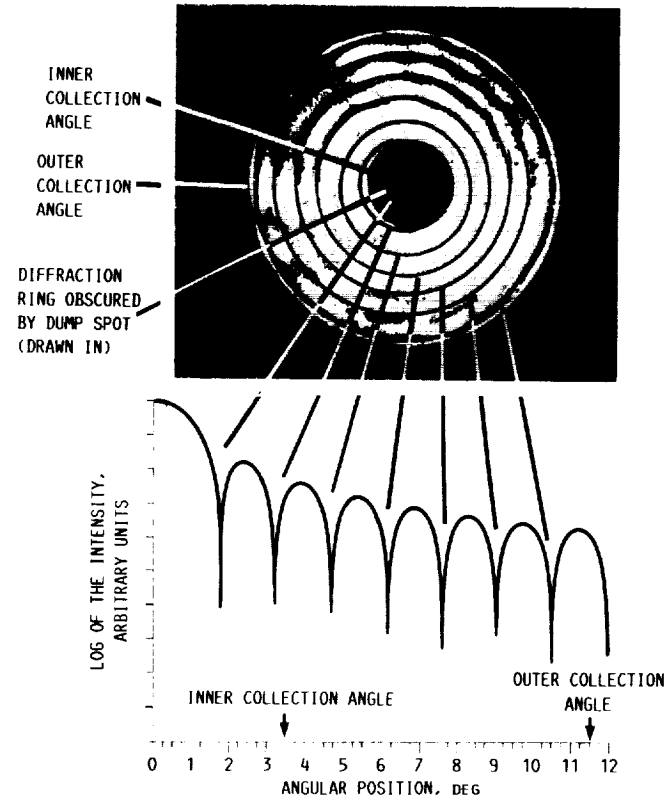


FIGURE 2.5. - DIFFRACTION PATTERN FROM A 25 μm PINHOLE USED AS A SCALE TO DETERMINE THE OPTICAL COLLECTION ANGLES.

Remove the photodetector module and the beam splitter from the photodetector box. In a darkened room, place a small mirror in the photodetector box and project the diffraction pattern onto a piece of paper taped to the wall. This will act as a screen. Figure 2.4 shows what this pattern will look like. As shown in the figure, the dump spot that is located on the FSSP's 90° prism as well as the diffraction rings should be visible. If the rings in the diffraction pattern look fuzzy, then reposition the pinhole (in the radial direction) within the beam. If the dump spot is not centered in the diffraction pattern (as in fig. 2.4) then the beam is not aligned on the dump spot. The laser mount has positioning screws to change the alignment if needed. Caution must be used when doing this because centering the beam on the dump spot can cause other optical components to become misaligned.

After the pinhole has been positioned, and the diffraction pattern is of sufficient quality to discern the rings, mark the center of the pattern and trace out the shadow of the dump spot. Next, mark the bright and dark rings on the paper and trace out the outer edge of the diffraction pattern. Remove the piece of paper from the wall. Note whether there are any rings obscured by the shadow of the dump spot. This can be determined from the spacing of the other rings. Next, locate the edge of the dump spot shadow and determine how many rings out from the center it is. This is the inner collection angle. Now, locate the outer edge of the diffraction pattern. This is the outer collection angle. Figure 2.5 is a plot showing the relationship between the diffraction rings and their angular location. On this particular instrument the inner and outer collection angles are at about 3.5° and 11.5°.

Certain electronic characteristics of the FSSP also need to be known. For example, when using a number density correction algorithm (ref. 4) to correct for counting losses due to instrument dead time, the electronic delays in the FSSP must be known. There are two delays in the instrument, the short delay for droplets outside of the depth of field, and the long delay for droplets inside the depth of field. To measure these delays, a signal must be generated at both the signal detector and the annulus detector. This can be done either with an electronic pulse generator (refs. 2 and 5) or with a rotating pinhole (described in the calibration section of this report). To measure the short delay, be sure the pulse amplitude at the annulus detector is larger than the amplitude at the signal detector (Do the inverse to measure the long delay). A good place to monitor the delays is at the pulse height analyzer in the FSSP. In the pulse height analyzer there are leads to monitor the transit time gate signal and the reset signal.

Look at both of these signals on an oscilloscope while injecting the electronic pulse into the detectors. The time difference between the end of the transit time gate and the peak of the reset signal is the delay period. Figure 2.6 shows the pattern on the oscilloscope trace when determining the short delay and the long delay. The two delay times for this instrument are 1.58 and 5.57 μ sec respectively.

Use of a pulse generator to inject signals into the FSSP in order to measure the instrument's electronic characteristics is adequate for most applications but there are two disadvantages. First, a certain amount of electronic noise is present when using this method. Occasionally the noise can affect the measurement. Secondly, the signal is always injected

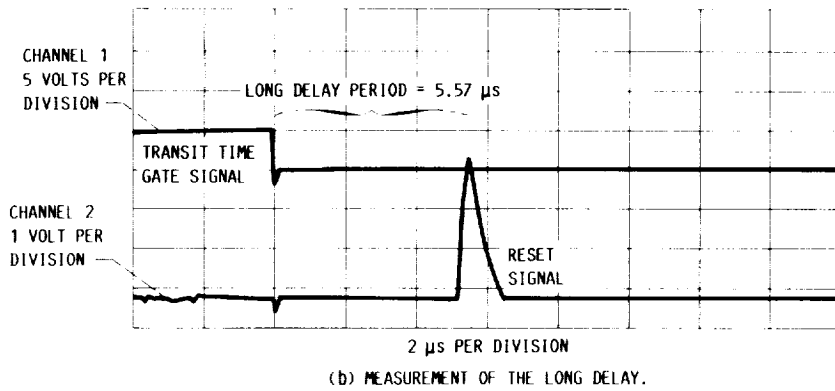
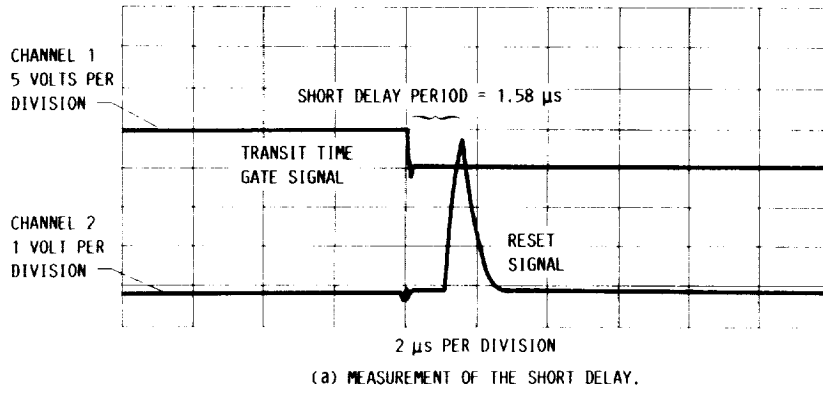


FIGURE 2.6. - MEASUREMENT OF DELAY TIMES IN THE FSSP.

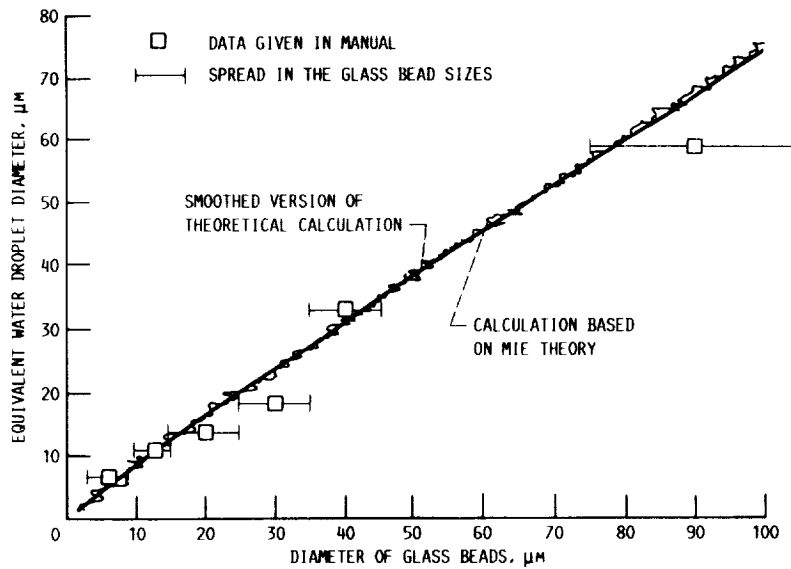


FIGURE 3.1. - TRANSFER FUNCTION RELATING GLASS BEAD DIAMETER TO WATER DROPLET DIAMETER IN THE FSSP.

downstream of the photodetector. Thus any problems with the photodetector will not be seen.

The alternative to using electronic signals is to use light pulses. One way to produce the required light pulses is with an acousto-optic modulator (AOM or Bragg Cell). This device is placed in a laser beam and can be used to modulate the beam. The modulation is controlled by a pulse generator. Thus, by sending a laser beam through the AOM and onto the FSSP's photodetector, light pulses of varying frequency, amplitude, and width can be produced. The advantages of this method are (1) low noise (there is no electronic coupling between the signal source and the FSSP), and (2) the signal is injected at the very start of the electronic system in the FSSP -- the photodetector.

One use of the AOM is to measure the electronic response of the FSSP. This is to determine how well the FSSP will measure short duration pulses. This is analogous to sending high velocity droplets through the laser beam, since they too will generate short duration pulses. Results of this test are in the section entitled, "Accuracy of the FSSP".

The measurements above must be made with the FSSP disassembled in the lab. There is one quite useful measurement that can be done in-situ. This involves monitoring of the signal and annulus detector voltages during flight or wind tunnel tests. Since this is not a feature on the FSSP, it must be added by the user. The advantage of such a feature is that it allows the instrument's response to be monitored in real time with an oscilloscope. As droplets go through the laser beam they scatter light onto the detectors. The oscilloscope monitoring these detectors will show a pulse each time a droplet goes through the beam. Monitoring the detectors in this way provides continuous information about signal quality, droplet number density and velocity, and cloud variability in real time.

Installation of the monitoring circuit in the FSSP should be done in such a manner as to not affect the normal operation of the instrument. One possible location is after the baseline restoration module in the FSSP. In NASA's FSSP, two wires are connected to the two lines that contain the signal voltage and the annulus voltage at this module. The two lines are also connected to unity gain follower circuits. The output of the follower circuits are connected into the standard FSSP data cable. On the NASA Lewis FSSP there are also two wires on the data cable that are not used; so no new external wires are needed to carry the signals back to the oscilloscope. These wires lead back to the control room, where the data acquisition system is located, and the proper two wires are connected to an oscilloscope. The signals at the scope can be noisy because the length of wire is several meters. Nevertheless, this simple circuit has proven to be quite useful.

3. CALIBRATION OF THE FSSP

There are several devices available for calibration of the FSSP. The advantages and disadvantages of each will be examined. The calibration devices reviewed will be (1) glass beads, (2) the droplet generator and (3) a new calibration device: the rotating pinhole.

3.1 Glass Beads

The most widely used method of calibration is to pass glass beads of a known size through the FSSP. Since the light scattered by a glass bead is of a different intensity than the light scattered by a water droplet of the same diameter, a transfer function is needed relating glass bead diameter to an equivalent water droplet diameter. The FSSP manual gives a limited version of the transfer function. In the manual, a plot shows the FSSP's response to various diameter glass beads. When the user checks the calibration, beads of the same size as those shown in the manual should give the same response.

A more detailed plot showing the response of the FSSP (in terms of an equivalent water droplet diameter) as a function of glass bead diameter is shown in figure 3.1. The points on the curve were generated by calculating the scattered light intensity from a glass bead of a given diameter and then calculating the diameter water droplet that gave the same intensity. The curve is multivalued because different diameter water droplets can scatter the same light intensity. The smoother curve represents the "best fit" of the multivalued one. Also included in this plot are the experimental data from the manual. Note that only horizontal error bars are plotted. These represent the spread in the true size of the glass beads. Spread in the measured size would be plotted with vertical bars, but this data is not given in the manual.

Advantages of using glass beads include their availability, ease of use, and optical similarity to water droplets. Glass beads are commercially available for calibration purposes. Sending the beads through the instrument's laser beam is relatively easy by using a vacuum hose and several attachments available from the manufacturer.

The optical similarity of glass beads to water droplets can be seen in figure 3.2. The figure compares the scattered light intensity as a function of glass bead diameter with the scattered light intensity as a function of water droplet diameter. The two curves are quite similar for diameters below 10 micrometers then diverge somewhat for larger droplets. Since the curve for glass beads falls below that of water droplets, larger diameter glass beads are needed to scatter the same amount of light as smaller diameter water droplets. When using substitute particles (such as glass beads or latex spheres) for calibration, the particle diameter cannot exceed the size range of the instrument. This is because for larger particles, the finite size of the laser beam begins to affect the instrument response. This effect is difficult to calculate and is not considered in any calibration curves for the FSSP. Using this size criterion it can be seen from figure 3.1 that when calibrating an FSSP with an upper size limit of 47 μm , the largest size glass bead used for calibration should be about 47 μm . This corresponds to a measured size of 36 μm . Thus, glass beads can be used for calibration over about 3/4 of the range of the FSSP. This is quite acceptable for most applications.

The disadvantages of the glass bead method are cost of the beads, the spread in the sizes, the quality of the beads, and control over the trajectory of the glass beads. Since a portion of the beads is lost each time a calibration check is made, they constantly need replacing. This can amount to a significant cost if detailed calibration studies are conducted. Also the

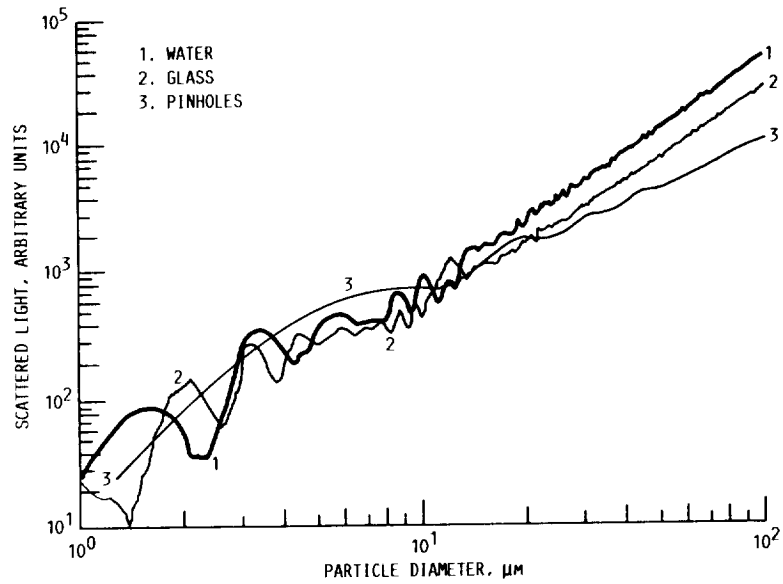


FIGURE 3.2. - COMPARISON OF THEORETICAL CALIBRATION CURVES IN THE FSSP.

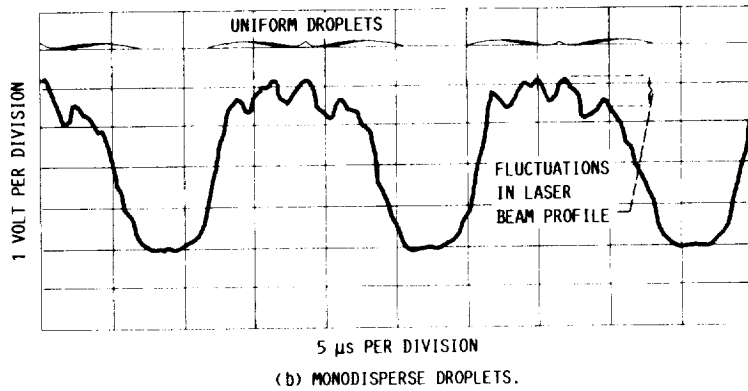
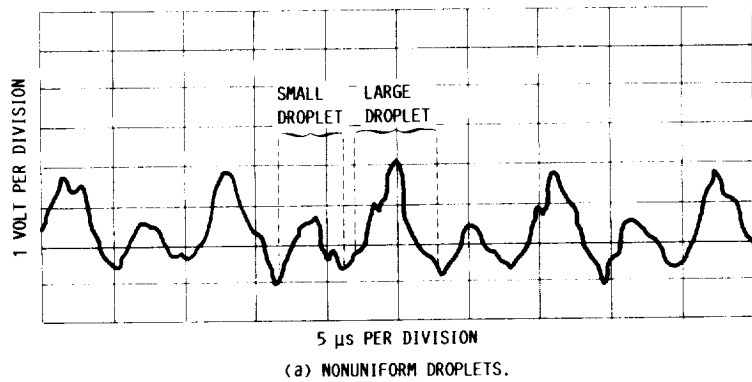


FIGURE 3.3. - SIGNAL GENERATED BY DROPLETS CROSSING THE PROBE VOLUME IN THE FSSP.

glass beads are not monodisperse, they have a spread in their true size (as shown by the horizontal bars fig. 3.1). This leads to uncertainty when calibrating the FSSP. The user does not know whether the instrument or the calibration sample is responsible for the spread in the measured size. Also the quality of the glass beads can be questionable. The beads can be chipped, broken, have air bubbles in them, or clump together. Also, when doing detailed calibration studies where the response of the instrument as a function of particle trajectory is of interest, glass beads are inappropriate because their trajectory is not easily controlled.

3.2 The Monodisperse Droplet Generator

For a number of years a vibrating orifice droplet generator has been commercially available and widely used for calibration. The device is intended to produce a single stream of droplets of a known size. It is good for some applications but it too has shortcomings.

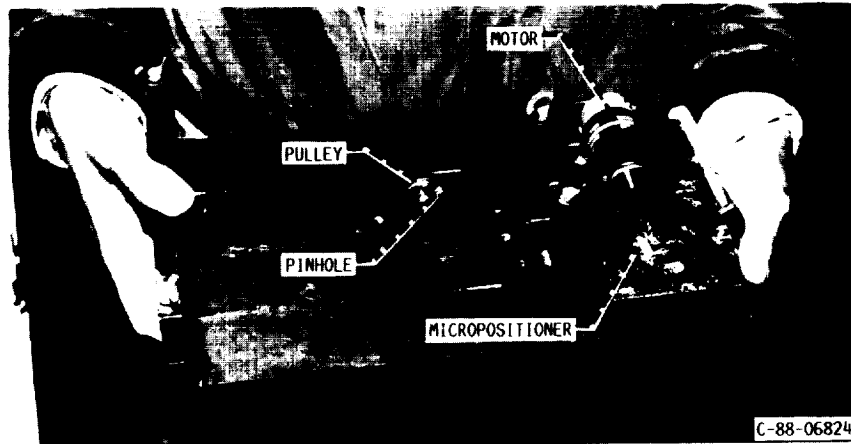
The major advantage for using the droplet generator is that it uses water droplets. This means that no transfer function is needed and calibration could "theoretically" be carried out over the entire range of the FSSP. Also, the single stream of droplets makes it possible to control the trajectory of the stream through the laser beam.

There are several problems that may be encountered when using this system for calibration of the FSSP. First, the droplet generator is intended for use in the laboratory and therefore it is not appropriate for calibration during wind tunnel or flight tests. It can be difficult to adjust the instrument to get a stable stream. The spray head can clog or become degraded over a short period of time, fluctuations in water pressure or air currents can send the droplet stream in unpredictable directions, and the supply syringe always seems to run out of water at the most inopportune times. Also, the droplet generator usually puts out droplets that are very close together, which can cause coincidence errors in the FSSP.

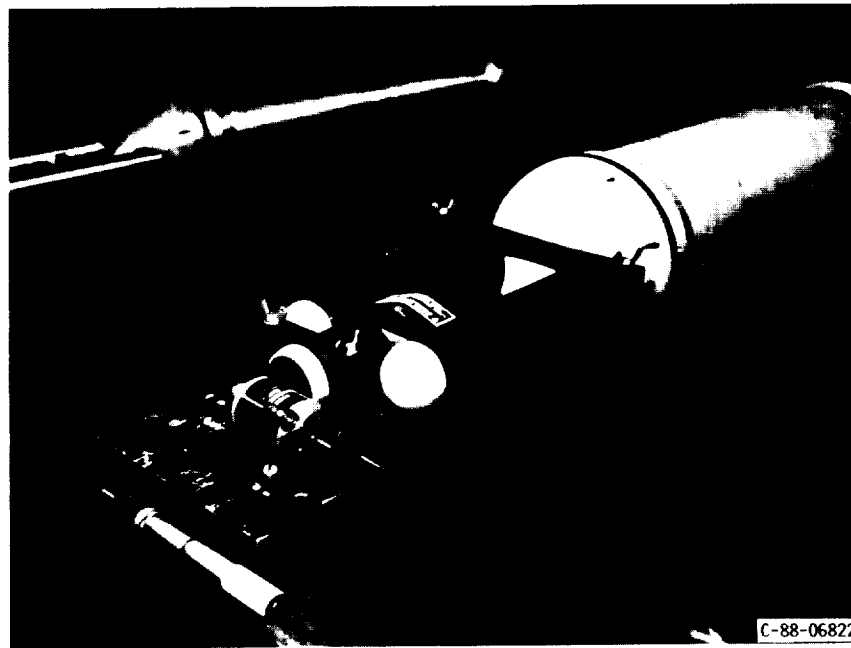
Even with these problems the nondisperse droplet generator is useful when performing some laboratory tests on the FSSP. For example, it is the only device that can perform a calibration check of large diameter droplets in the extended range FSSP (5- to 95- μm range).

There are several modifications that may be helpful when using the droplet generator. To solve the pressure fluctuation problem, a pressurized water tank is used instead of the syringe. Since the tank is much larger than the syringe, the supply will last all day even while constantly spraying. The large tank also keeps down the number of times the tank will need refilled. Thus, dirt has less of a chance of entering the system and causing clogs. The flow rate can be measured by collecting a water sample for several minutes in a small graduated cylinder or weighing the sample on a microbalance. The fluctuations in the droplet stream can be minimized by getting the spray head as close as possible to the laser beam. This is best accomplished by removing the flow straightening tube on the FSSP. The uniformity of the droplet stream is easily monitored by observing the voltage (on an oscilloscope) coming from the signal detector. Figures 3.3(a) and (b) show oscilloscope traces depicting nonuniform and uniform droplet streams. Note that in figure 3.3(a) the particles traversing the beam are alternately large then small. In figure 3.3(b) the droplets are all of one size and the FSSP will group 90 percent of

ORIGINAL PAGE
BLACK AND WHITE PHOTOGRAPH



(a) COMPONENTS OF THE CALIBRATOR.



(b) CALIBRATOR ATTACHED TO FSSP.

FIGURE 3.4. - THE ROTATING PINHOLE CALIBRATOR.

these droplets into one size bin. Also note in figure 3.3(b) the uneven signal (fluctuations between 3 and 4 V). This reveals the uneven illumination of the laser beam as the droplet passes through regions of varying intensity.

3.3 The Rotating Pinhole -- A New Calibration Device

A new calibration device developed at NASA Lewis is the rotating pinhole. This has proven quite useful in both laboratory and field tests. As with the previous calibration devices, it has advantages as well as limitations.

The rotating pinhole is, as its name implies, a device which rotates a calibration pinhole through the laser beam of the FSSP. It consists of a motor attached to a belt and pulley system (see fig. 3.4(a)) which rotates a pinhole (calibration pinholes are commercially available). The entire system is mounted on a two-axis micropositioning table so the precise trajectory of the pinhole through the beam can be controlled. The entire assembly is easily slid on and off of the probe arms of the FSSP without removing the flow straightening tube (see fig. 3.4(b)).

The principle of operation of the rotating pinhole is as follows. Pinholes of a given diameter diffract light. The intensity of this light can be calculated. A pinhole of a given diameter, when rotated through the laser beam, will cause a predictable response in the FSSP. If the response is other than the predicted value, then the FSSP is out of calibration.

As with glass beads, the diameter of a pinhole is related to the diameter of a water droplet by using a transfer function calculated with Mie theory. This function is shown in figure 3.5. The curve is multivalued for the same reason as the glass bead transfer function. The "best fit" curve is also plotted in figure 3.5. This figure shows the expected FSSP response as a function of pinhole diameter. Several points from the figure 3.5 are listed in figure 3.6. This shows the FSSP response to several pinhole diameters that are commercially available.

There are several advantages to using the rotating pinhole both in the laboratory and in the field. First, the diameter of the pinhole is known to a high degree of accuracy. The pinhole is stable, durable, and a repeatable standard. The pinholes are reusable. Also, the pinhole trajectory is controlled easily for detailed laboratory work such as measuring the FSSP's depth of field, or the beam profile, or for troubleshooting instrument malfunctions.

During wind tunnel tests the rotating pinhole provides a quick method of checking out the instrument. The calibration can be verified in a matter of seconds. Small shifts in calibration due to misaligned optics or wet lenses are easily detected. The pinhole rotator can even help realign the FSSP as illustrated in figures 3.7(a) to (c). The oscilloscope traces in figures 3.7(a) to (c) show the voltage level (which is proportional to scattered light intensity) as a 15- μ m pinhole cuts through the laser beam. Channel 1 is coming from the signal detector and channel 2 is coming from the annulus detector. The misalignment shows up as an asymmetric signal coming from the annulus detector in figure 3.7(a). Overcompensation of the alignment setting

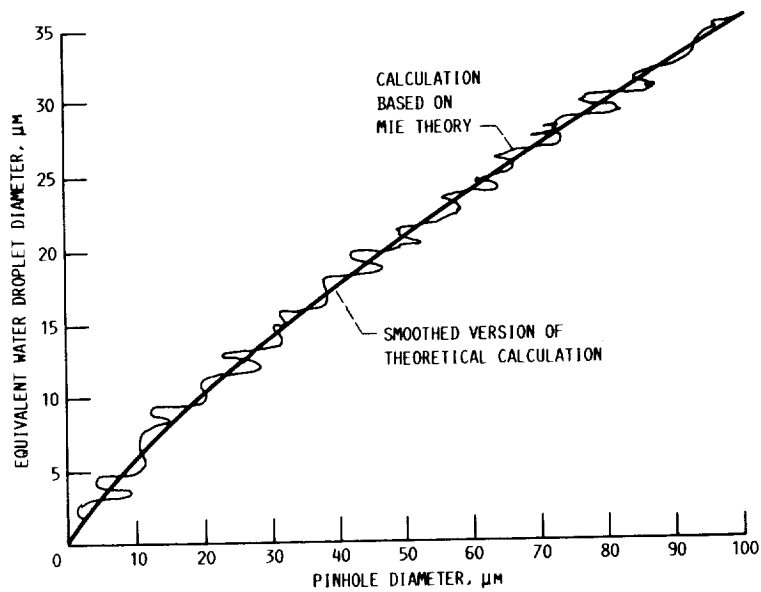


FIGURE 3.5. - TRANSFER FUNCTION RELATING PINHOLE DIAMETER TO WATER DROPLET DIAMETER IN THE FSSP.

Pinhole diameter, μm	FSSP response (equivalent water droplet diameter), μm
5	3 to 4
10	5 to 6
15	9 to 10
20	10 to 11
25	12 to 13
50	20 to 22
100	35 to 37

FIGURE 3.6 - THE FSSP RESPONSE TO SEVERAL COMMON SIZE PINHOLES.

is illustrated in figure 3.7(b). Proper alignment is shown in figure 3.7(c). Note the annulus detector remains at zero volts because it intercepts no scattered light as the pinhole rotates through the center of the depth of field.

There are two disadvantages to the pinhole rotator method. First, only the pinholes are commercially available at this time. However, if a user wishes to build the device, all the parts are standard catalog items. The other disadvantage is that the light diffracted by the pinhole is much less intense than that scattered by a water droplet of the same diameter as was shown in figure 3.2. This means large size pinholes are needed to calibrate the FSSP. As mentioned previously, laser beam diameter becomes an important factor when using any large-size particle or pinhole. The largest size pinhole that should be used with the FSSP should not be bigger than the largest size droplet the instrument is designed to measure. Thus, for instruments whose range ends at 47 μm , a 47- to 50- μm pinhole is the largest pinhole that should be used. From figure 3.6 this corresponds to about a 20- μm water droplet. This means that the rotating pinhole is appropriate for calibration of less than half of the total range of the FSSP.

3.4 Comparison of the Various Calibration Techniques

Calibration checks were done at NASA Lewis with an extended range FSSP by using glass beads, the pinhole rotator, and a water droplet generator. The results show an interesting trend.

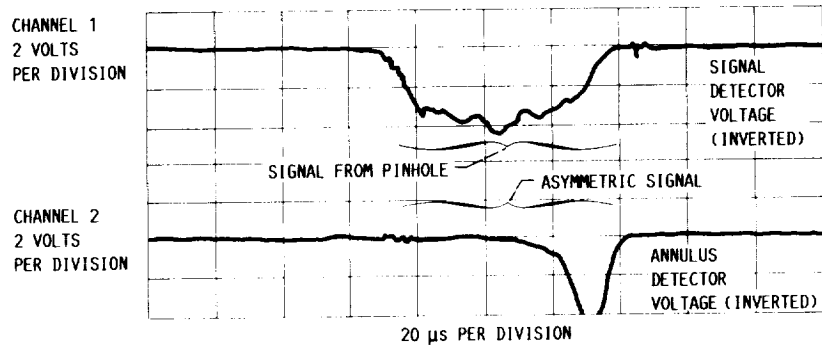
Plotted in figure 3.8 are the FSSP's theoretical response to glass beads, a calibration done at NASA Lewis using glass beads, and the manufacturer's experimental data from the manual. There are two points to note: (1) the spread in the true size of the glass beads (horizontal error bars) makes calibration uncertain, and (2) the instrument seems to undersize large particles.

Plotted in figure 3.9 are the FSSP's theoretical response to pinholes and the FSSP's measured response to several pinhole diameters. Horizontal error bars are not necessary because there is no variability in pinholes' diameter. Note that as with the glass beads, the largest particles appear to get undersized.

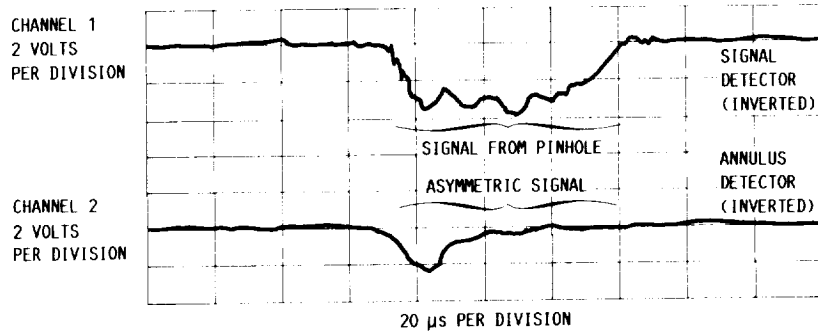
FSSP calibration data using the droplet generator represents only one data point. This data is shown in figure 3.10. The measured distribution is sharply peaked, thereby indicating the droplets were monodisperse. A quantity of 4.47 ml of water was collected over 4 min and the frequency at which the droplets were being produced was 54107 droplets per second. This indicates a size of 88 μm . Again the FSSP is undersizing large droplets. Reasons for the undersizing of large droplets will be addressed in the following section.

4. ACCURACY OF THE FSSP

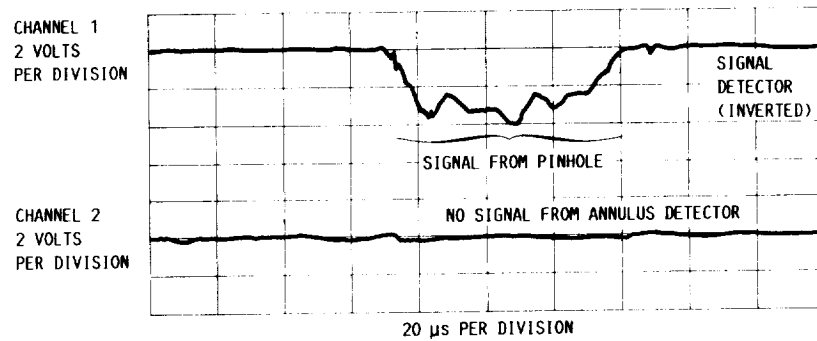
One of the most difficult aspects of particle sizing instrumentation is to quantify the errors associated with the measurement. The reason is that a cloud cannot be created in which the droplet size distribution is known to a



(a) OSCILLOSCOPE TRACE IDENTIFYING MISALIGNED OPTICS IN THE FSSP.



(b) OVERCOMPENSATION OF THE ALIGNMENT SETTING.



(c) A PROPERLY ALIGNED INSTRUMENT: NO SCATTERED LIGHT GOES INTO THE ANNULUS DETECTOR WHEN THE PINHOLE ROTATES THROUGH THE CENTER OF THE DEPTH OF FIELD.

FIGURE 3.7. - USING THE ROTATING PINHOLE TO ALIGN THE FSSP.

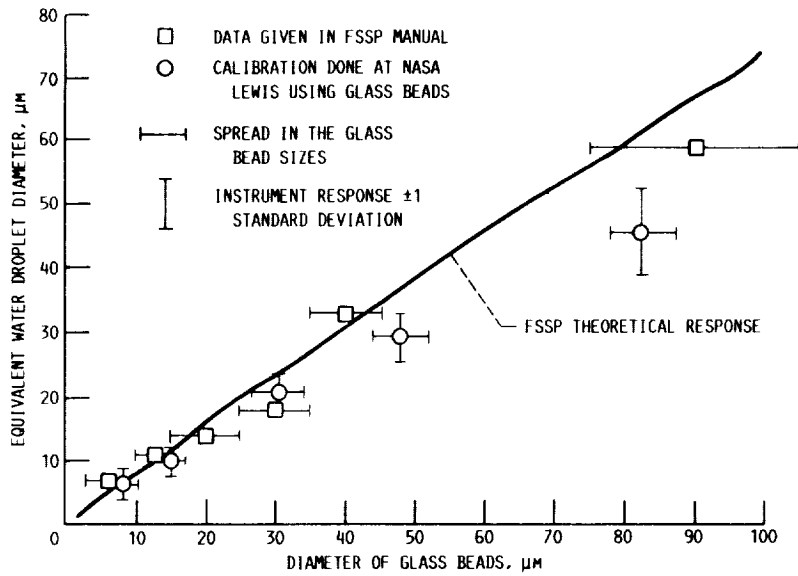


FIGURE 3.8. - CALIBRATION OF THE FSSP USING GLASS BEADS.

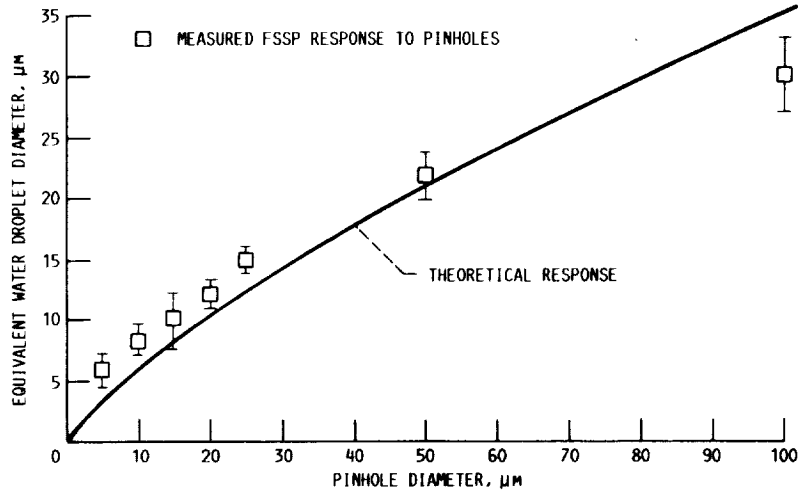


FIGURE 3.9. - CALIBRATION OF THE FSSP USING ROTATING PINHOLES.

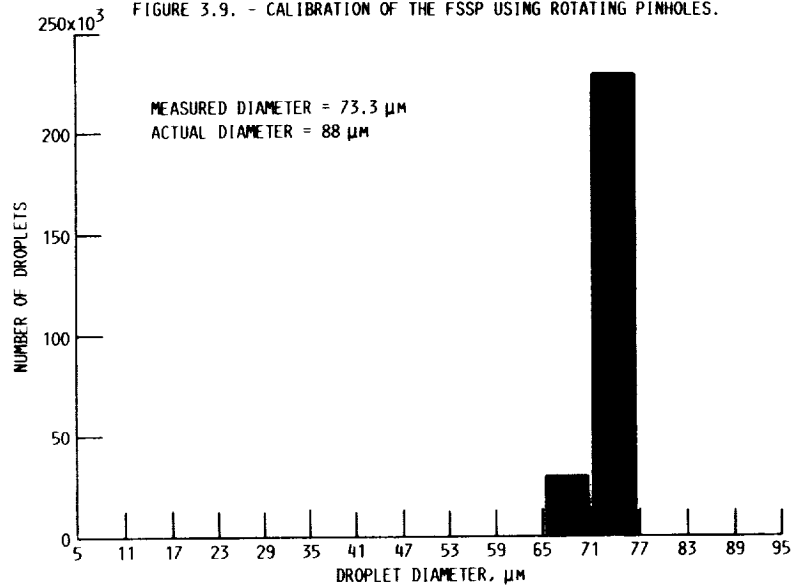


FIGURE 3.10. - DISTRIBUTION FROM A MONODISPERSE DROPLET GENERATOR.

high enough degree of accuracy to be used as a standard. Thus, assessment of the accuracy of an instrument like the FSSP must be done by testing each component of the instrument individually to determine sources of error. This method is far from reliable since it does not take into account the effects of one component interacting with another. One alternative to this type of testing is to conduct computer simulations. In this case the interaction between components can be modeled and overall accuracy can be determined. The drawback to this is that the simulation is only as good as the mathematical model of the instrument. Some aspects of the instrument are not practical to model. Another alternative is to compare the instrument with another one that uses a different principle of operation. The obvious limitation to this is the need for a more accurate instrument to compare with the one in question. All three of these methods were employed to assess the accuracy of the FSSP.

The following parameters were analyzed to determine the magnitude of the measurement errors they cause: number density of the cloud, flow velocity of the cloud, calibration errors, laser beam illumination and size-velocity correlation. Given these environmental conditions and instrument characteristics, the accuracy of the FSSP was assessed in terms of its ability to measure the average diameter (D_{10}), the median volume diameter (MVD), number density, and liquid water content.

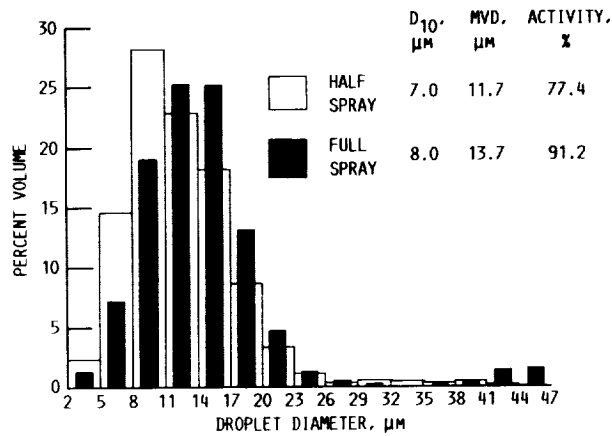
4.1 Number Density Errors

Errors in the FSSP that occur during conditions of high number density are difficult to quantify. It is true that counting losses caused by high number density have been documented and correction algorithms formulated (ref. 4). However, counting losses is not the only error that occurs during conditions of high number density. Sizing errors can also occur in the FSSP. Quantifying these sizing errors will be the emphasis of this section.

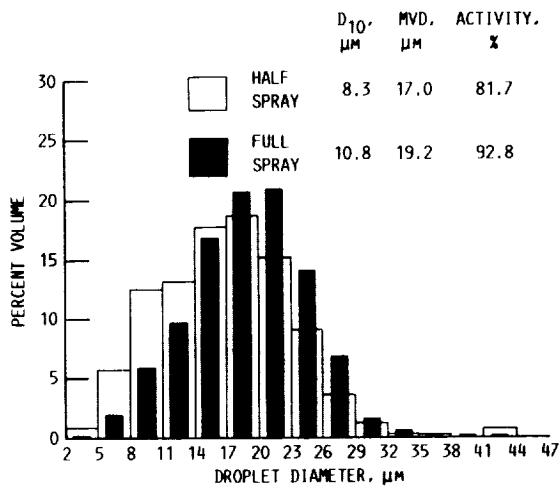
In order for the FSSP to make an accurate size determination, only one droplet at a time should be in the probe volume. However, multiple droplets are more likely to appear in the probe volume as number density increases. If multiple droplets are in the probe volume then a coincidence event occurs and a sizing error is likely. Additionally, droplets that are outside of the probe volume (yet in the laser beam) can cause sizing errors for a droplet that is in the probe volume. The magnitude of the error depends on the number of droplets in the entire laser beam, their position relative to the probe volume, their position relative to one another, and their size.

Coincidence events cause two kinds of sizing errors in the FSSP. The first error is a sizing bias. To understand the sizing bias, a sizing event must first be defined. A sizing event begins when a droplet enters the probe volume. It ends when the droplet leaves the probe volume. If another droplet enters the probe volume before the previous one left, then the sizing event continues until the second droplet leaves the probe volume. The sizing event is not over until all coincident droplets have left the probe volume. At the end of the sizing event the FSSP makes a size determination.

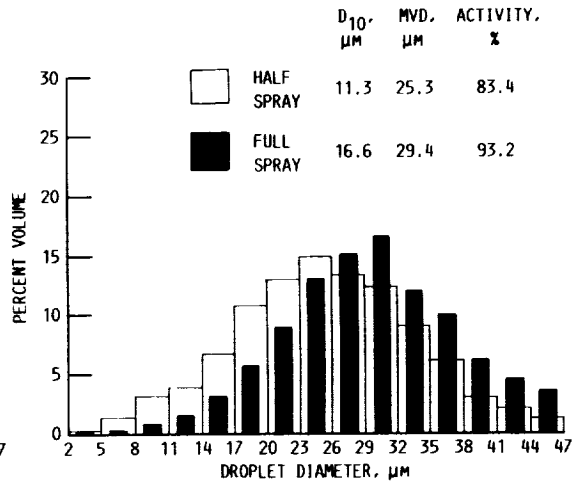
The size determination must be made when the droplet is totally illuminated by the laser beam and scattering is at a maximum. As the droplet leaves the laser beam the scattering decreases to zero. The signal detector produces a voltage pulse that is proportional to the intensity of the scattered



(a) A DISTRIBUTION AT THE BOTTOM OF THE SIZE RANGE.



(b) A DISTRIBUTION AT THE MIDDLE OF THE SIZE RANGE.



(c) A DISTRIBUTION AT THE TOP OF THE SIZE RANGE.

FIGURE 4.1. - COMPARISONS OF MEASURED DISTRIBUTIONS IN THE ICING RESEARCH TUNNEL.

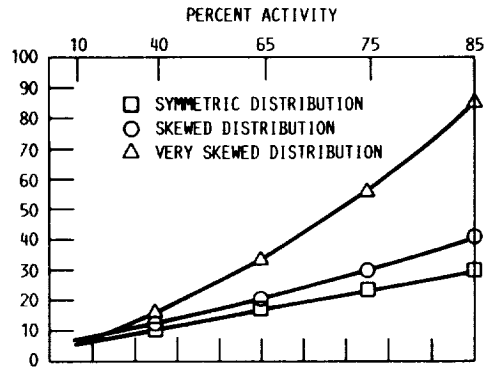
light as the droplet passes through the probe volume. The peak intensity or the peak voltage coming from the signal photodetector contains the size information about the droplet. Thus, only the peak voltage from the signal photodetector is used for making the size determination.

This method of using the peak voltage to make a size determination can cause a sizing bias if coincidence events occur. Consider a sizing event in which one droplet passes through the probe volume followed by another droplet that is much smaller. The FSSP will count these two droplets as one (a counting error) but more important, the measured size will always correspond to the size of the larger droplet. This is because the peak voltage will always correspond to the larger droplet. This is true no matter which order the droplets go through the probe volume. In this type of sizing event, the largest droplet is always sized and the smaller ones are always ignored. If the number density is high enough to cause coincidence events to occur frequently, the FSSP will bias the distribution toward the larger droplets.

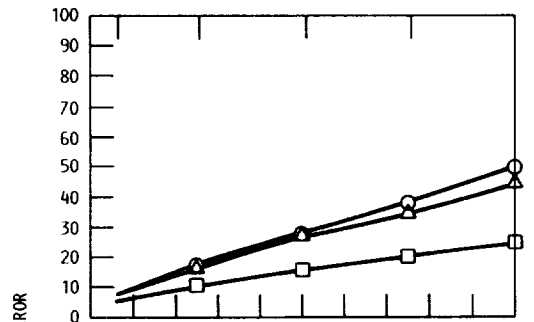
The second type of coincidence event causing a sizing error occurs when the light scattered by multiple droplets in the laser beam combine to cause the signal to be more intense than any one droplet alone. This causes the FSSP to measure several smaller droplets as one larger one.

An experiment was conducted in the NASA Lewis Icing Research Tunnel (IRT) which gives a qualitative example of the sizing error that can occur during conditions of high number density. In the IRT there are eight spray bars each containing 10 to 15 nozzles for a total number of 100 nozzles. In the experiment a series of test conditions were run in the tunnel that caused the activity (ref. 1) of the FSSP to be in excess of 90 percent. This indicated conditions of high number density. It was suspected that coincidence events were causing sizing errors in the FSSP. To check this, the same conditions were repeated, except every other spray bar was shut down and only 50 nozzles were used to spray water. It was assumed this caused a reduction in the number density without affecting the distribution shape. If this assumption is correct then any differences between the measured distributions were caused by coincidence errors. Comparison of three measured distributions ("full spray" versus "half spray") are shown in figures 4.1(a) to (c). This data gives a qualitative example of sizing errors that can occur during conditions of high number density. Note that in each case the measured distribution was skewed to the right when number density was higher (full spray). This caused the average diameter and the MVD to be larger when the number density was larger.

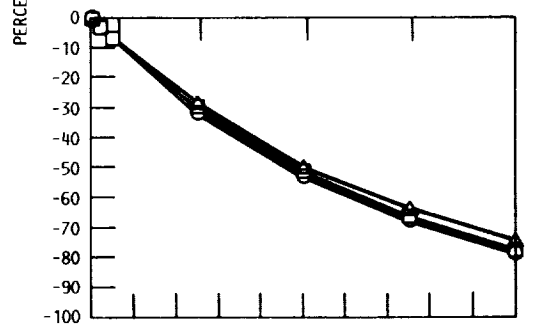
Quantifying sizing errors caused by coincidence events is difficult using mathematical models. Testing in the laboratory is also difficult because the true number density is always uncertain. To quantify this error, a computer program was written to simulate the operation of the FSSP. The simulation models almost every aspect of the FSSP: beam diameter, depth of field, signal and annulus detector response as a function of droplet position and velocity, and the Mie scattering response function. Two aspects about the instrument were simplified for practical reasons. First, all the droplets are treated as point sources of scattered light. Second, the simulated laser beam profile is different than the true laser profile, which is very irregular and impossible to model exactly. The profile in the simulation has the gross features of the FSSP's laser beam but is much smoother. It is assumed that these two simplifications will have a minimal influence on the calculations.



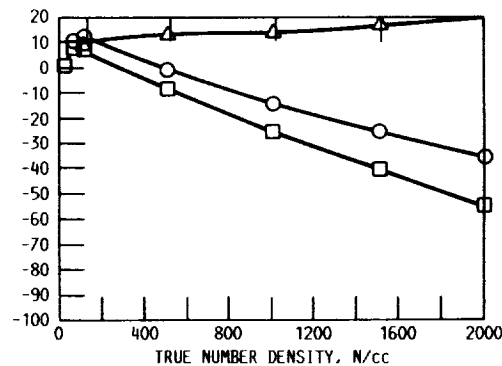
(a) ERROR IN THE MEASURED AVERAGE DIAMETER.



(b) ERROR IN THE MEASURED MEDIAN VOLUME DIAMETER.



(c) ERROR IN THE MEASURED NUMBER DENSITY.



(d) ERROR IN THE MEASURED LIQUID WATER CONTENT.

FIGURE 4.2. - COINCIDENCE ERRORS BROUGHT ON BY HIGH NUMBER DENSITY. (DATA FROM COMPUTER SIMULATION.)

The magnitude of sizing errors caused by high number density will vary from instrument to instrument depending primarily on the beam diameter and the depth of field of the instrument. For the simulation the beam diameter was set at 220 μm and the depth of field was 2 mm. Also, the simulation assumed the instrument was in perfect calibration. Figure 4.2(a) shows the computed error in the measured average diameter as a function of number density. Figure 4.2(b) shows the computed error in the median volume diameter as a function of number density. Note that the error is always positive, thereby indicating the FSSP would oversize the droplets. The various curves on the plots show the computed error when different distribution shapes were assumed. The squares represent a symmetric distribution centered in the range, the circles represent a mildly skewed distribution, and the triangles represent a very skewed distribution that is peaked at the bottom of the range.

Also of interest in this simulation is the error in measured number density and liquid water content as a function of true number density. Figures 4.2(c) and (d) show these results. Figure 4.2(c) shows the computed error in the measured number density. Note that error is always negative, indicating undercounting from the simulated FSSP. This error is due to counting losses and has been documented by other researchers (ref. 4).

The error in the measured liquid water content (LWC) is caused by a combination of the sizing error (due to coincidence events) as well as the counting losses. The first effect tends to cause the instrument to measure LWC higher than the true value, while the second causes the measured LWC to be lower. These two effects show up in figure 4.2(d). For the droplet size distributions corresponding to the symmetric and mildly skewed cases (squares and circles), sizing errors dominate and the LWC error is positive when the number density is less than 100 per cubic centimeter. Then the error goes negative for higher number densities because counting losses dominate. For the case of the highly skewed distribution (triangles in fig. 4.2) where the sizing error is large, the counting losses never dominate and the error stays positive.

Although the error is a function of instrument parameters and the droplet size distribution, this simulation should give some idea as to the sizing accuracy of the FSSP in conditions of high number density.

4.2 Velocity Errors

Measurement errors caused by high velocity droplets have been previously documented (ref. 5). For NASA's extended range FSSP, measurement of the expected error as a function of velocity was conducted with the use of an acousto-optic modulator. Optical pulses of a very short duration were sent into the signal detector of the FSSP to simulate rapidly moving particles. A plot showing the FSSP's response as a function of optical pulse width is given in figure 4.3. Also plotted is the equation $y = 1 - \exp(-t/t_0)$, where t_0 is the instrument response time of 0.53 μsec . The plot shows that there will be virtually no sizing errors unless the width of the optical pulse is less than 1.6 μsec . This plot can be used to estimate velocity dependent sizing errors in the FSSP. For example if the FSSP's beam diameter is 200 μm and the droplets are traveling at 100 m/sec relative to the instrument, then the longest optical pulse (corresponding to a droplet going through the center of the laser beam) will last 2 μsec . Since some droplets will go through the

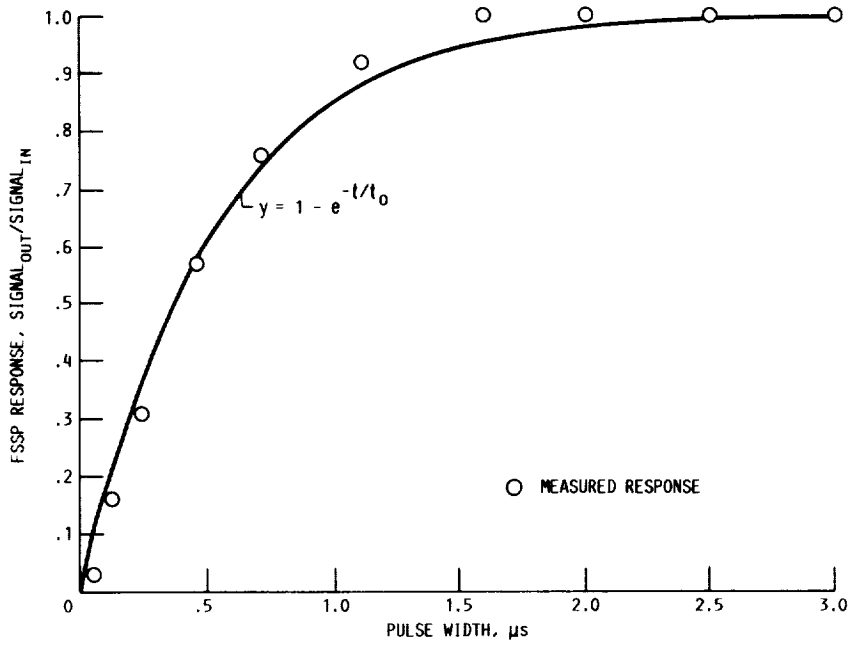


FIGURE 4.3. - FSSP RESPONSE TO SHORT DURATION OPTICAL PULSES.

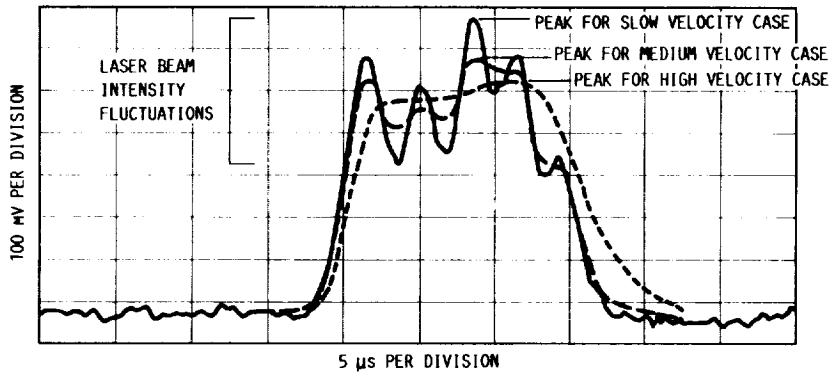


FIGURE 4.4. - FSSP RESPONSE FOR A 5-μm PINHOLE MOVING AT 10 m/s AND THE ESTIMATED RESPONSE FOR FASTER VELOCITY PARTICLES.

edge of the beam, they will produce shorter duration pulses. On the average the duration of the pulses will be 0.78 times the duration of the longest pulse or 1.56 μm . (0.78 is the average chord length through a unit diameter circle.) From figure 4.3 it can be seen that 1.56 μsec corresponds to a sizing error of about 5 percent.

While a 5-percent estimation of the error is representative of the error for larger droplets ($>50 \mu\text{m}$), it does not represent a complete picture of the velocity dependent sizing error. When small droplets traverse the probe volume of the FSSP they pass through regions of varying intensity. If the droplet is moving at a slow velocity then the FSSP can resolve these intensity fluctuations. This is shown in figure 4.4 for a 5- μm pinhole moving at approximately 10 m/s. The peak intensity occurs when the pinhole (or water droplet) goes through a bright region of the laser beam. This is proportional to the measured size of the particle. As the velocity increases, the FSSP is not able to respond to these rapid oscillations in the intensity. This is depicted in figure 4.4 for medium and high velocity particles. Since the pinhole cannot be rotated at aircraft velocities the responses shown for the medium and high velocity cases are estimated.

Figures 4.3 and 4.4 can be used to estimate the sizing error of a 5 μm droplet moving at 100 m/s. The width of the laser beam intensity fluctuations shown in figure 4.4 are about 10 percent of the width of the entire beam. If a 200- μm laser beam and a velocity of 100 m/s is assumed then the duration of the intensity fluctuations are 0.2 μsec . With the data in figure 4.3, 0.2 μsec corresponds to a decrease in intensity of about 80 percent. This means the small scale intensity fluctuations will be poorly resolved. This is depicted as the high velocity case in figure 4.4. Comparing the peak intensities for both the low and high velocity cases yields a sizing error of about 20 percent.

4.3 Calibration Errors

The FSSP has a calibration curve defined internally by its electronic circuitry. This "instrument calibration curve" is set by the manufacturer and is determined both experimentally (with glass beads) and theoretically (with the Mie scattering theory) (ref. 1). The instrument calibration curve is essentially a model of how water droplets in the FSSP scatter light. Any differences between this model and the way water droplets actually scatter light in the FSSP, will cause errors in the measured diameter of the droplets. These errors are called calibration errors. Two types of calibration errors will be discussed in this section. First to be discussed are errors that occur when measuring large droplets ($>50 \mu\text{m}$) in the extended range FSSP. The second error to be examined is caused by small droplets of different diameters that scatter the same amount of light.

The ability of the FSSP to measure large droplets is governed by the diameter of the laser beam in the probe volume. With a larger beam the FSSP can more accurately measure a larger droplet. This is because the instrument calibration curve for the FSSP is based on Mie theory, which assumes the water droplet is evenly illuminated. If the droplet is too large for the probe volume, then parts of the droplet will always be in dimmer regions of the beam. The water droplet will scatter less light than Mie theory predicts and

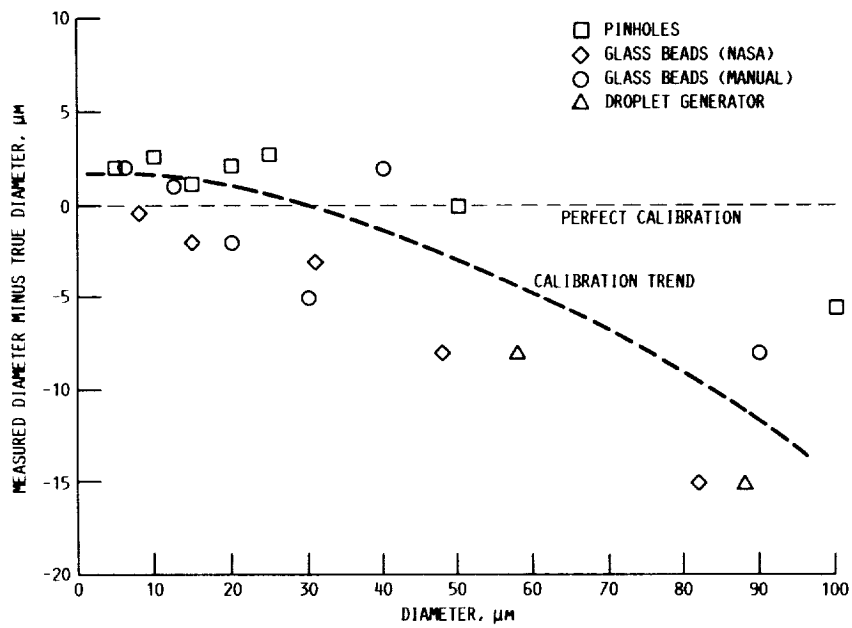


FIGURE 4.5. - CALIBRATION ACCURACY OF THE NASA LEWIS EXTENDED RANGE FSSP.

the instrument will undersize the droplet. Increasing the diameter of the laser beam is not practical because it increases the probe volume and increases the likelihood of coincidence events. Developing a modified version of Mie theory to take into account the uneven illumination of large droplets is not possible at this time because of the complexity of such a theory. Thus, the only way to estimate the error is experimentally.

The accuracy of the FSSP can be estimated for large droplets by comparing the FSSP to other instruments, by using rotating pinholes, and by using glass beads. The data for all of these methods is shown in figure 4.5. The data shows the absolute error (measured size minus true size) for NASA's FSSP. The data was taken less than a year after the recommended annual factory calibration. The data shows that this FSSP undersizes large particles by about 10 to 15 μm .

This calibration error may account for the discrepancy between the FSSP data and that of another particle sizing instrument (the Phase Doppler Particle Analyzer, Aerometrics, Inc.). Data in figure 4.6 was taken at Arnold Engineering Development Center's Icing Wind Tunnel. The Phase Doppler and the FSSP made simultaneous measurements at nearly the same location in the tunnel. The probe volume of the Phase Doppler instrument was directly in front of the flow straightening tube on the FSSP. In figure 4.6(a) there is a discrepancy between the two distributions, most notably in the large sizes or the tail of the distribution. In this region the Phase Doppler instrument typically measured many more droplets than the FSSP. If the Phase Doppler is assumed to be accurate, then this indicates the FSSP has a serious sizing problem when measuring large droplets. It is not known if this is a problem that is unique to this particular FSSP or if it is a fundamental problem characteristic of all extended range FSSPs. If it is a fundamental problem, then this is important to icing researchers because the tail of the size distribution contributes most to the MVD.

Further comparisons were made between the FSSP and the Phase Doppler instrument in the 2- to 47- μm range of the FSSP. This range is often used by icing researchers. Comparisons using this range are shown in figure 4.6(b). Agreement is better when using this range. The mode (or peak) of the distributions agrees exactly in most cases. However, if the distribution has a tail, then the agreement between the two instruments becomes worse as shown in figure 4.6(c).

Another calibration concern is the multivalued nature of the theoretical calibration curve for small droplets. Droplets of different diameters can scatter the same amount of light. In figure 4.7 the theoretical Mie scattering calibration curve is plotted along with the actual instrument calibration curve for the 1- to 16- μm range (as given in the FSSP manual). Note that the instrument curve is a smoothed approximation to the theoretical one. The best calibration curve (representing the way water droplets actually scatter light in the FSSP) is probably a combination of both curves; that is, not as irregular as the theoretical curve and not as smooth as the instrument curve. The shape of the curve also depends on the size of the droplet. The theoretical curve is probably a better approximation for smaller droplets. This is because Mie scattering theory assumes that the droplet is evenly illuminated. A small droplet, by virtue of its size, is more likely to be evenly illuminated than a larger one.

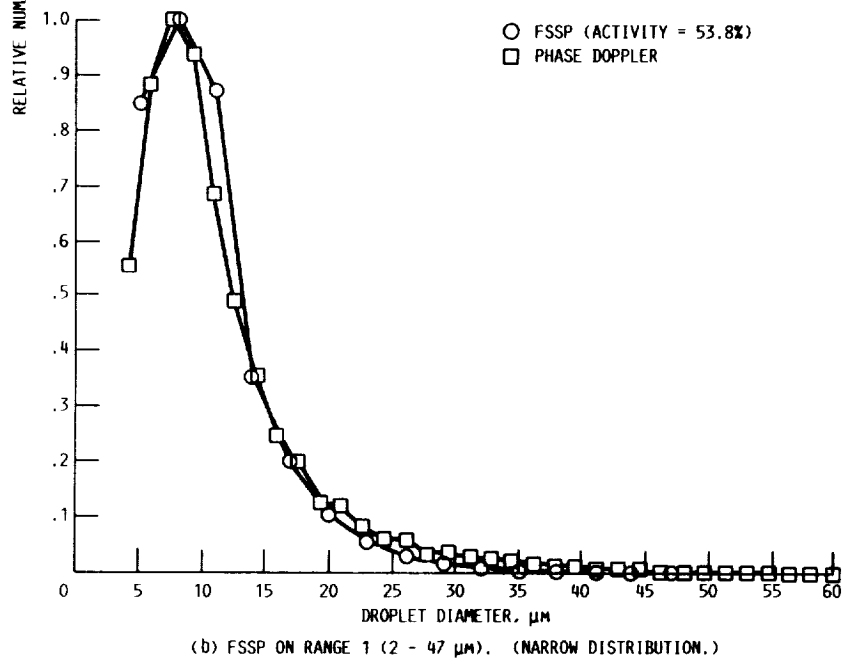
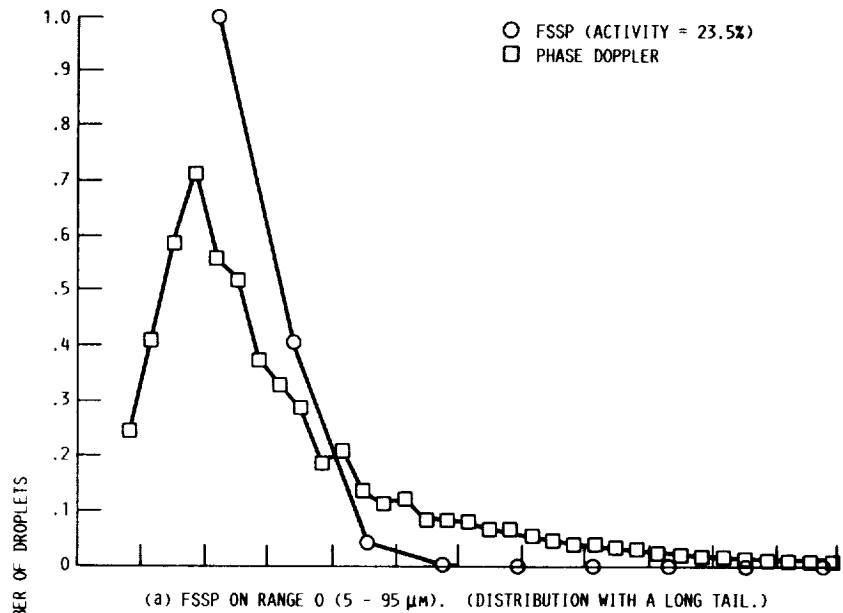
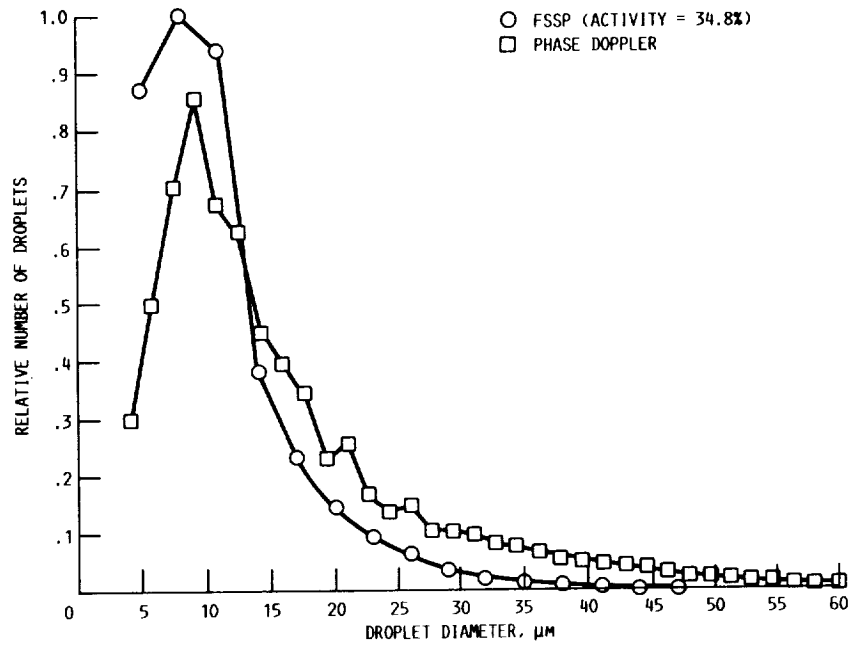


FIGURE 4.6. - COMPARISONS BETWEEN THE FSSP AND THE PHASE DOPPLER PARTICLE ANALYZER.



(c) FSSP ON RANGE 1 (2 - 47 μm). (DISTRIBUTION WITH A LONG TAIL.)
 FIGURE 4.6. - CONCLUDED.

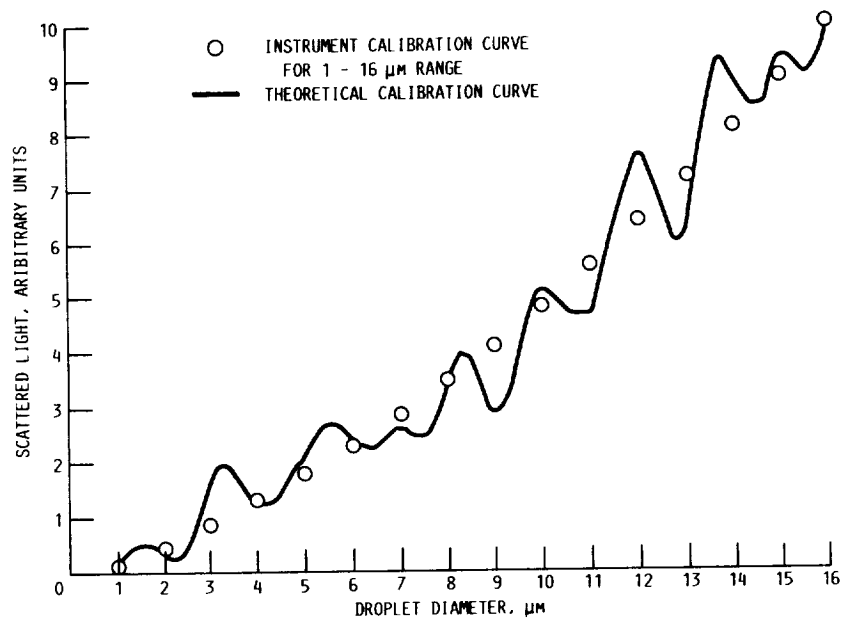


FIGURE 4.7. - THEORETICAL CALIBRATION CURVE COMPARED WITH INSTRUMENT CALIBRATION CURVE.

To quantify the error caused by the irregular nature of the calibration curve, a computer simulation was used. Input into the simulation was the actual calibration curve of the FSSP, the theoretical curve, and a distribution of small droplets. The simulated response was computed and compared with the input distribution. The difference between the input and computed distributions represents a "worst case" prediction of the error. Figure 4.8 shows the comparison for this one case. The distribution is distorted. The 6- to 7- μm bin is most notably distorted. Even with the distortion, the average diameter and the MVD differ from the input distribution's average diameters by less than 2 percent. It should be noted that no other instrument effects were modeled so that any differences are due entirely to the irregular calibration curve.

If these errors in the distribution are unacceptably large then redefinition of the size bins is a method to correct this. Reference 6 gives details of how to change the bin boundaries to accommodate the multivalued nature of the Mie response curve. This method can also be used to correct for undersizing of the large droplets.

4.4 Laser Beam Illumination Errors

The trajectory of a droplet through the FSSP's probe volume can affect the measured size of the droplet. This is due to an uneven laser beam illumination in the probe volume. If two identical droplets go through different regions of the probe volume that have different illuminations, then the FSSP will measure them differently. The one that goes through the more intense region will be sized as a larger droplet. This kind of error causes a broadening of the size spectrum or spectral broadening: droplets that should be grouped into one size bin are instead grouped into adjacent bins.

Before quantifying the spectral broadening error, it is informative to see the cross section of the FSSP's beam at the center of the probe volume (fig. 4.9). Data for this plot was generated by rotating a 5- μm pinhole through the center of the FSSP's laser beam. The voltage at the signal detector was read by a storage oscilloscope and transferred to a computer. The time dependent voltage measured by the oscilloscope represented a one-dimensional intensity profile of the beam. The pinhole was then repositioned to cut across another chord of the beam and process was repeated many times. The one-dimensional slices were then assembled into the two-dimensional plot of the intensity profile shown in the figure.

Figure 4.9 clearly shows the uneven illumination within the probe volume. However, these fluctuations in the laser beam illumination change with increasing pinhole (or droplet) diameter. This is because larger diameter particles tend to average over the intensity fluctuations in the beam. Figures 4.10(a) to (d) show this for 5-, 25-, 50-, and 100- μm pinholes. Note that the intensity fluctuations for the 5- μm pinhole have an amplitude that is about 40 percent of the peak intensity, while the fluctuations for the 100- μm pinhole are only about 5 to 10 percent of the peak intensity. This data indicates that uneven laser beam illumination is not a serious problem with larger size droplets.

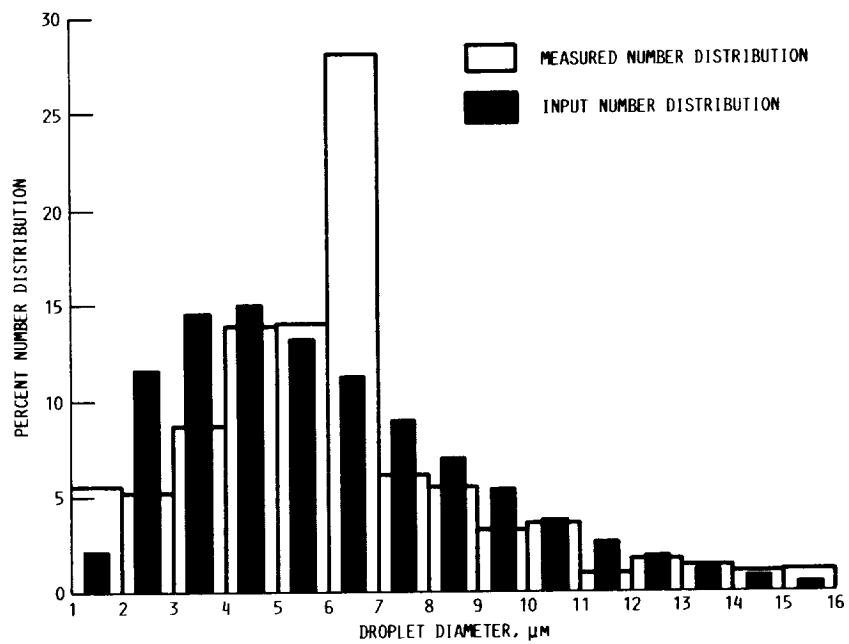


FIGURE 4.8. - SIMULATION TO EVALUATE CALIBRATION ERRORS.

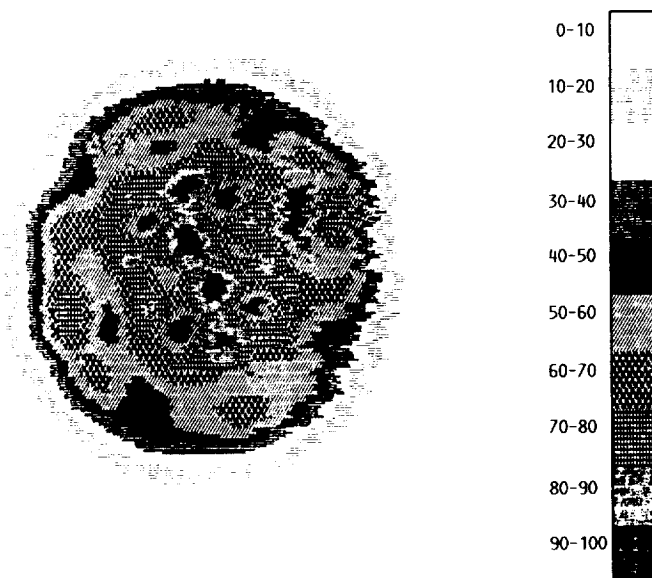
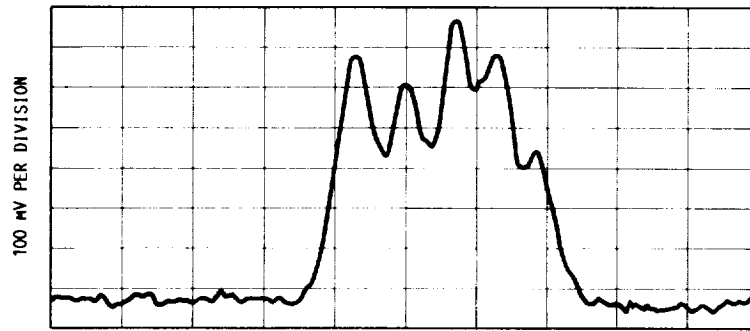
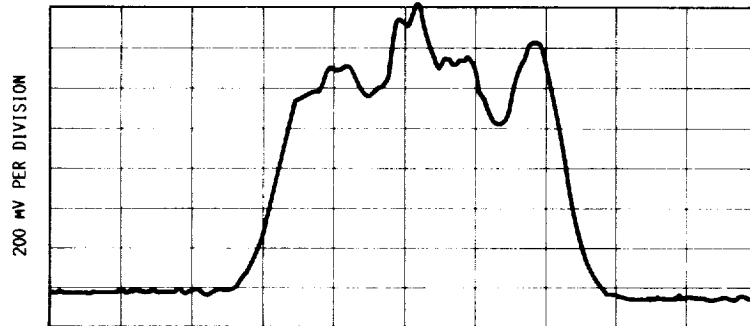


FIGURE 4.9. - INTENSITY CROSS SECTION OF THE FSSP LASER BEAM.

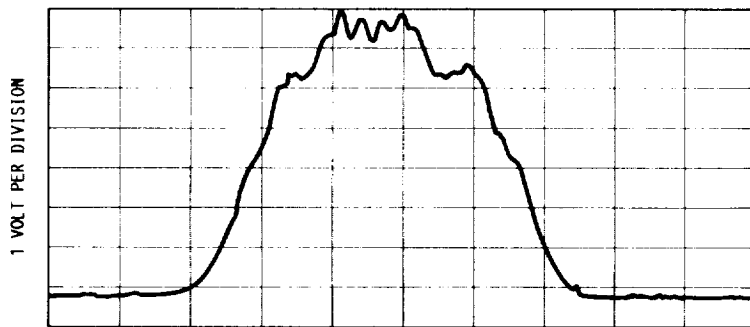
ORIGINAL PAGE
BLACK AND WHITE PHOTOGRAPH



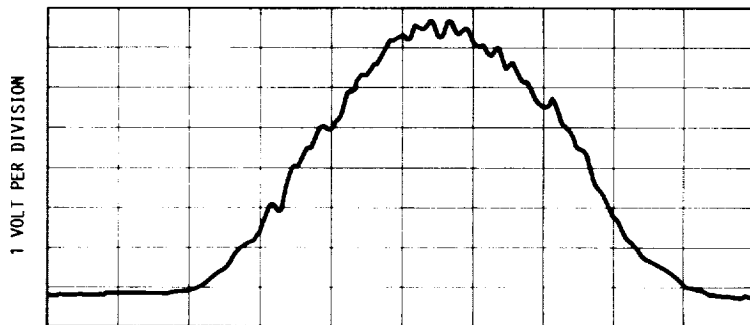
(a) A 5 μm PINHOLE.



(b) A 25 μm PINHOLE.



(c) A 50 μm PINHOLE.



5 μs PER DIVISION
(d) A 100 μm PINHOLE.

FIGURE 4.10. - INTENSITY FLUCTUATIONS FOR VARIOUS DIAMETER PINHOLES CROSSING THE PROBE VOLUME.

Quantifying the error caused by the uneven illumination was done experimentally. Again, a rotating pinhole was used to do this. The experiment was done in two stages. First, a pinhole was rotated through the probe volume along the same trajectory. The trajectory used was the one that produced the maximum signal (this was usually very close to the radial center of the beam). The second stage of the test used the same pinhole except it was rotated through varied trajectories of the probe volume by means of a computer-controlled positioner. Comparison of the two tests reveals the effect of uneven illumination.

Figure 4.11 compares the results of the two tests. Note that there is increased broadening of the size spectrum when the pinhole goes through varied trajectories. This is attributed to the uneven laser beam illumination in the probe volume. The magnitude of the broadening for this size pinhole is about $5\ \mu\text{m}$ or 5 bins when operating the FSSP on the 1- to 16- μm range (bin widths are $1\ \mu\text{m}$ in this range). When the instrument is operated on less sensitive ranges, like the 2- to 47- μm range (which has 3- μm bin widths), the broadening is still $5\ \mu\text{m}$, but this corresponds to a broadening of only one or two size bins. Thus the effect of uneven laser beam illumination will be most evident when the instrument is being operated in the most sensitive size range.

To quantify the effect of broadening on a realistic droplet size distribution, a model of the broadening is needed. Such a model was formulated based on the data given in figure 4.11. The model is a spectral broadening algorithm that takes droplet counts from one size bin and distributes them in adjacent bins. A graphical representation of the model is shown in figure 4.12. Applying this spectral broadening algorithm to a more realistic distribution will give an estimation of the error it causes in the FSSP. Figure 4.13 shows the input distribution with the shaded bars and the same distribution distorted by the spectral broadening algorithm with the wider bars. Note that the distortion is not as prominent as when the input distribution was monodisperse. Also note that the error in the MVD and the error in the average diameter is less than 1 percent for this distribution. Assuming this model is an accurate representation of spectral broadening in the FSSP, then one can expect errors of about 1 percent when operating the FSSP on the 1- to 16- μm range. In the size ranges with wider bins the error will be negligible.

4.5 Size-Velocity Correlation Errors

All of the droplets the FSSP measures in any given sample must be traveling at the same velocity. This is because the FSSP accepts or rejects droplets depending on the droplet's transit time through the laser beam. Recall that droplets with a short transit time are rejected because it is assumed they went through the edge of the laser beam and could have been sized incorrectly. If a size-velocity correlation exists (droplets of one size are moving at a different velocity than those of another size) then a velocity bias error is possible.

This error occurs when the FSSP biases the measured distribution toward slower moving droplets because those droplets will be in the laser beam for a longer period of time than faster ones. Thus the transit time circuit in the FSSP rejects more of the faster moving droplets. If the faster moving droplets correspond to a given size class of droplets, then that size class will be

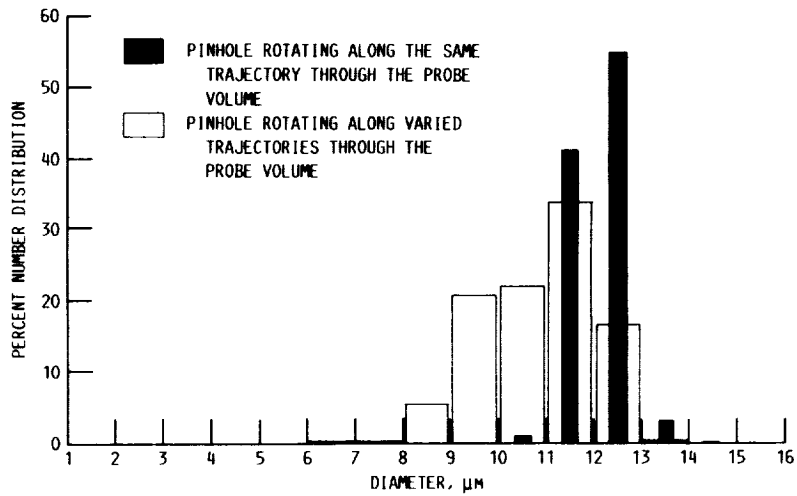


FIGURE 4.11. - FSSP DATA SHOWING BROADENING OF THE SIZE DISTRIBUTION WHEN A PINHOLE IS ROTATED ALONG VARIED TRAJECTORIES THROUGH THE PROBE VOLUME.

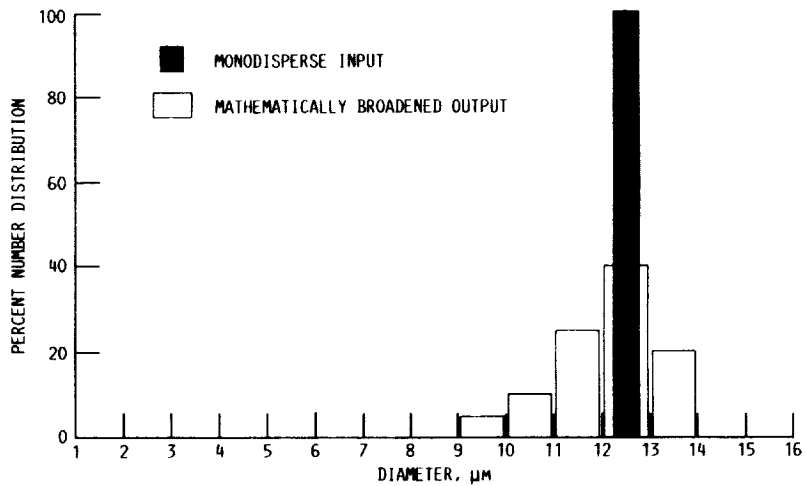


FIGURE 4.12. - GRAPHICAL REPRESENTATION OF THE SPECTRAL BROADENING ALGORITHM.

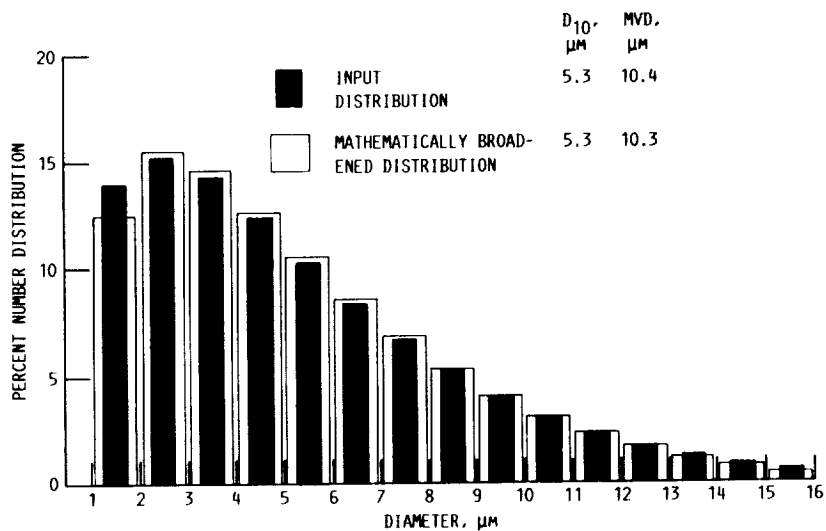


FIGURE 4.13. - SIMULATION SHOWING EFFECTS ON THE SIZE DISTRIBUTION CAUSED BY UNEVEN LASER BEAM ILLUMINATION.

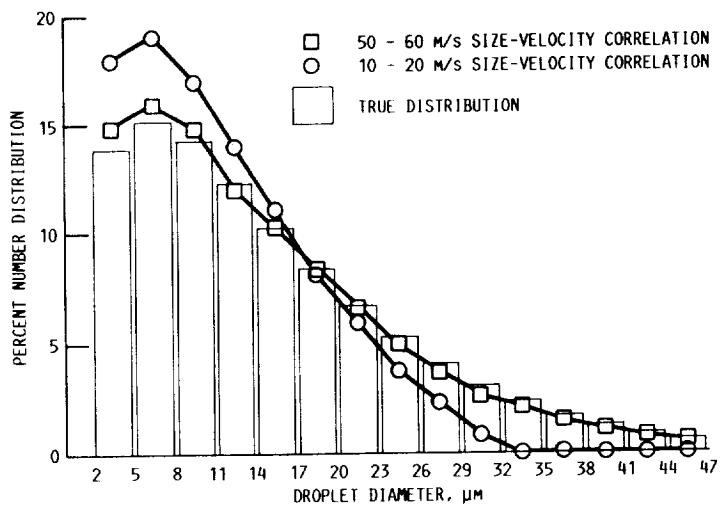


FIGURE 4.14. - SIMULATION DATA SHOWING THE EFFECT OF SIZE-VELOCITY CORRELATION IN THE FSSP.

undercounted. For example, assume that an FSSP is in perfect working order, is calibrated perfectly, and will make no sizing errors. Also assume the cloud that the FSSP is to measure contains large droplets that are moving fast and small droplets that are moving slow. Then this ideal FSSP will measure a distribution that will be skewed toward the small end of the size spectrum and the average diameter and MVD will be measured smaller than the true value.

It should be noted that the velocity bias error discussed here is not the same as the sampling differences caused by temporal versus spatial sampling (ref. 7). Those sampling differences also cause a measurement bias and are also caused by a size-velocity correlation (the bias is toward faster moving droplets). These sampling differences have been previously analyzed and documented, and an algorithm has been formulated to relate one type of sampling to the other (ref. 8). The error discussed in this section is unique to the FSSP and biases the distribution toward the slower moving droplets.

A size-velocity correlation could occur in many circumstances: proximity to spray nozzles, turbulence from the aircraft, or any source of turbulence. Even turbulence caused by the body of the FSSP can change the flow field. Some calculations have been performed and preliminary indications show the effects may be significant (ref. 9). It is beyond the scope of this report to analyze or quantify the various causes of size-velocity correlation. Instead, a size-velocity correlation will be assumed, and the velocity bias error it causes in the FSSP will be calculated.

A size-velocity correlation and a droplet size distribution was assumed and input to the FSSP simulation program previously discussed. The droplets at the small end of the distribution had slower velocities than those at the large end. To make certain no other effects caused a sampling bias, other errors intrinsic to the FSSP were not modeled. Figure 4.14 shows the effect of the size-velocity correlation. In figure 4.14 the true distribution (bar graph) is compared with the measured distributions when two different size-velocity correlations were assumed. The filled squares represent the simulated FSSP response when the small droplets were moving at 50 m/s and the large ones at 60 m/s (the velocity varied linearly with diameter). The filled circles represent the simulated FSSP response when the small droplets were moving at 10 m/s and the large ones at 20 m/s (again the velocity varied linearly with diameter). In the 50- to 60-m/s case the size-velocity correlation caused a negligible error (less than 5 percent) in the measured average diameter and the MVD. In the 10- to 20-m/s case the size-velocity correlation caused a 20- to 30-percent error in the measured average diameter and the MVD.

4.6 Overall Accuracy of the FSSP

The overall accuracy of the FSSP is dependent on the particular instrument and the measurement conditions. Thus, one single number cannot be given as "the error". The alternative is to list the types of errors and the factors that cause them, then estimate each error based on wind tunnel tests, laboratory experiments, and computer simulations. This data is given in figure 4.15. (Keep in mind that these errors were estimated based on the plots

Type of error	Important factors	Range where error occurs	Error
Calibration sizing error	Size of droplets	0 to 50 μm 50 to 100 μm	$\pm 5 \mu\text{m}$ up to 10 μm
Number density sizing error (oversizes)	True number density Sample volume size Droplet size distribution	0 to 100 per cm^3 100 to 500 500 to 1000	5 percent 5 to 10 percent 10 to 30 percent
Number density counting error (undercounts)	True number density Sample volume size	0 to 100 per cm^3 100 to 500 500 to 1000	5 percent 5 to 25 percent 25 to 50 percent
Uneven laser illumination sizing error	Droplet size distribution Laser beam profile Instrument range	1 to 16 μm >16 μm	1 to 2 percent negligible
Size-velocity correlation sizing error	Strength of correlation	All sizes	5 to 30 percent
Probe volume uncertainty counting error	Instrument alignment	All sizes	10 to 15 percent
Velocity sizing error (undersizes)	Velocity of cloud Instrument response Droplet size	100 m/s	5 to 20 percent

FIGURE 4.15 - THE OVERALL ACCURACY OF THE FSSP.

and data given in this section and will vary depending on the many factors discussed in this report.)

5. OPERATION OF THE OPTICAL ARRAY PROBE

5.1 Theory of Operation

The Optical Array Probe (OAP) is an optical particle sizing instrument that measures the diameter of particles by using an imaging technique. When a droplet passes through the laser beam in the OAP, a lens system transfers the image of the particle onto a linear array of photodetectors. When the image or shadow of the particle passes over individual elements in the photodetector array, the intensity decreases. If the intensity decreases more than 50 percent, then it is assumed the photodetector is within the shadow of the particle. After the particle passes through the laser beam, the number of photodetectors that experienced a 50-percent drop in intensity are counted. This number is proportional to the diameter of the particle.

As with the FSSP, the OAP must reject particles that are outside of its probe volume because they may be sized incorrectly. The OAP determines the probe volume by determining the degree to which the particle is in focus. To determine the degree of focus of a particle, the OAP assesses the drop in intensity each of the photodetectors experienced while the particle passed through the laser beam. If any of the photodetectors experienced a drop of 66 percent or more, then the droplet is assumed to be in focus enough to make an accurate size determination.

The OAP must also reject particles whose edges are off of the photodetector array. To do this the OAP makes a check of the two photodetectors that are at either end of the array. If either end photodetector is in the shadow of the particle (i.e., experiences a 50-percent drop in intensity) then it is assumed that the particle extends beyond the range of the photodetector array. If this happens, the particle must be rejected because it would be undersized.

5.2 Measurement of Optical Characteristics

Two OAP optical characteristics are its depth of field and its counting probability. The depth of field refers to the axial position along the laser path where particles are in focus enough to be measured. The counting probability is the probability that a particle will in be the probe volume and get counted. The counting probability depends on particle diameter.

The depth of field in the OAP needs to be characterized because particles that cross the laser beam at different locations along the depth of field are measured with varying degrees of accuracy. Particles are within the depth of field if they pass the 66-percent threshold test discussed above. In order to characterize the instrument's response to particles at different locations within the depth of field, a rotating reticle was used (refs. 3, 10, 11, and 12). The reticle provides a means of sending pseudo-particles (chrome disks deposited on a glass substrate) along precisely known trajectories through the laser beam. Details about the reticle will be discussed in the OAP calibration section.

For the depth of field test, the reticle was attached to a motor and the motor was attached to a two-axis micropositioning table. As the reticle rotated, the entire apparatus (reticle and motor) moved slowly up and down so the image of the chrome disk cut across the photodetector array at different locations. Data was taken with this procedure at one location within the depth of field. After several minutes of taking data, the average diameter measured by the OAP was calculated, and the reticle was moved to another location in the depth of field. This continued until the average measured diameter at each location in the depth of field was known. A plot showing the average diameter as a function of depth of field is shown in figure 5.1. The data is for three different reticle spot sizes: 50, 100, and 150 μm in diameter. Note that the OAP measures the diameter most accurately when the reticle disk is in the center of the depth of field. This is the region of best focus. As the reticle disk moves farther from the region of best focus, it can be undersized or oversized with an error of about 15 percent. This effect tends to cause a broadening of the size distribution.

The other characteristic about the OAP that affects accuracy is the counting probability (this is referred to in the OAP manual as the effective array width). Not all particle sizes have an equal probability of being counted by the OAP. For example, a small particle's image can go over the photodetector array along many different trajectories and not trigger the end reject photodetectors in the OAP. Because of this effect, smaller particles have a large probability of being counted. On the other hand, a large particle's image must cross the photodetector array very close to the center of the array. Any deviation, from this path will cause the image to go over the end photodetectors and the particle will get rejected. This restricts the possible trajectories of larger particles and thus these particles have a smaller probability of being counted.

To quantify this counting probability, the rotating reticle and computer controlled micropositioner were again used. This time all measurements were made at the center of the depth of field. As before the rotating reticle was slowly translated. The translation caused the reticle's image to cut across the photodetector array at different positions. At times the image traveled across the center of the array and was counted. At other times the image cut across the edge of the array and was rejected. The quantity of interest was the number of counts registered by the OAP for each reticle size disk per unit time. This is proportional to counting probability. Figure 5.2 shows the data from this experiment. Note the probability goes to zero for reticle disks larger than 620 μm . The effective width of the detector array is 620 μm , thus particles larger than this will always trigger at least one of the end reject detectors and therefore can never be counted. The decrease in counting probability for increasing particle size was expected although a more linear decrease was anticipated. The nonlinearities turned out to be from systematic errors in the computer controlled positioner.

The important feature of figure 5.2 is the counting probability for particles less than 30 μm . These particles have a lower probability of being counted. This is likely caused by the spacing between the photodetectors in the array. The very small reticle disks (or particles) can cut across the photodetector array and not be counted if they go between the photodetectors in the array. This decreases the probability of counting small particles. This

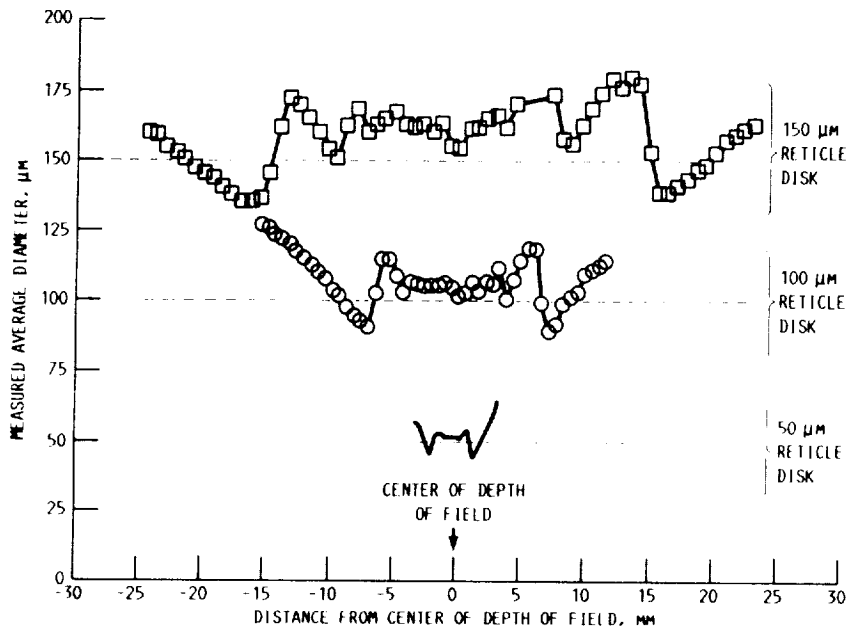


FIGURE 5.1. - MEASURED DIAMETER OF RETICLE DISKS AS A FUNCTION OF RETICLE POSITION IN THE DEPTH OF FIELD FOR THE OAP.

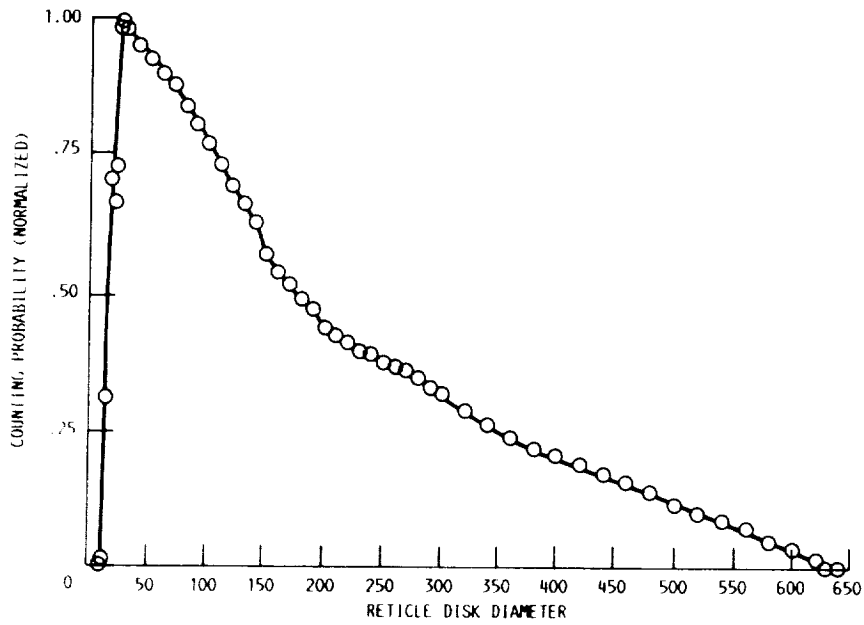


FIGURE 5.2. - COUNTING PROBABILITY IN THE OAP.

effect must be included in the data analysis to get an unbiased measurement of the particle size distribution.

6. CALIBRATION OF THE OAP

The rotating reticle has been developed for the Optical Array Probe as a calibration device. The reticle allows calibration in each of the 62 size bins in the OAP model 260X, and can be used for sample volume characterization if used with a micropositioner.

The reticle consists of a round glass disk 10 cm in diameter and 3 mm thick. Chrome disks of a known diameter are permanently deposited on the surface of the glass. The disks are arranged on the glass in concentric rings or tracks. The track used to calibrate the OAP consists of 64 disks varying in diameter from 10 to 640 μm .

To use the reticle for calibration of the OAP, several additional devices are needed. First, a small DC motor is needed to spin the reticle. Also an angle encoder is attached to the shaft of the motor so that as the reticle is spinning, the angular position of the reticle is known and thus the size of the disk in the sample volume of the OAP is also known. By using the angle encoder with an electronic timing circuit, a timing signal can be sent to the OAP. This signal is used to enable and disable the strobe line in the OAP. The effect is like turning on the OAP while the disk is going through the sample volume and turning off the OAP when the disk is not in the sample volume. There are two advantages for doing this. First, this allows selection of any one disk out of the 64 possible disks on the track. The second advantage is that this reduces the problem caused by dirt and dust specks that can collect on the reticle. Since the OAP is only active when a disk is going through the sample volume, dust will not cause any interference unless it is very close to the disk. This seldom occurs because the disks and the area around them comprise such a small fraction of the total area on the reticle surface. The disadvantage of using the timing circuit is that it requires a slight modification of the OAP's strobe line.

Figure 6.1 shows the calibration curve for the OAP. The straight line represents perfect calibration (1:1). The various symbols represent the counts the OAP detected in the various size bins. The filled squares are for bins with more than 50 percent of the counts, the circles are for bins with 5 to 50 percent of the counts, and the dots are for bins with 0 to 5 percent of the counts. Although the data does show some spill over into adjacent bins, the bin containing most of the counts is almost always on the line of perfect calibration.

The rotating reticle is very good for calibration of the OAP. It gives detailed results (calibration in every size bin throughout the entire range); it can be used to map the response of the OAP as a function of depth of field; it can be used to determine the counting probability; and it is currently commercially available (ref. 13).

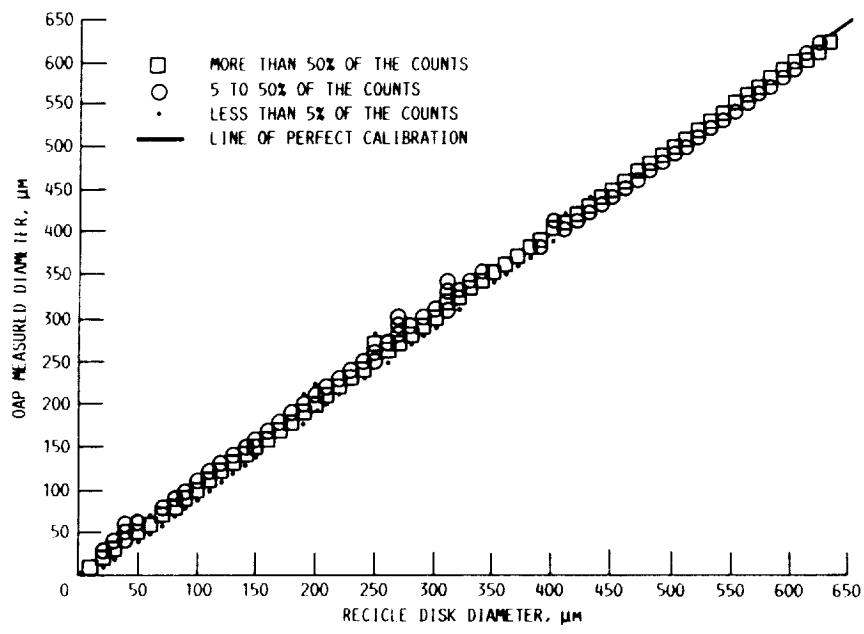


FIGURE 6.1. - CALIBRATION CURVE FOR THE OAP USING THE ROTATING RETICLE.

7. ACCURACY OF THE OAP

The calibration curve previously shown in figure 6.1 certainly makes the OAP seem to be very accurate throughout its entire range. It is true that the OAP (when properly calibrated) can accurately measure reticle disks when they are rotated through the center of the sample volume. However, there are other factors to consider when accessing the accuracy of the OAP. These include the counting probability, broadening of the size distribution due to out of focus particles, coincidence errors, velocity errors, and statistical uncertainties (the effect of a small number of particles in the tail of the distribution). Except for the velocity errors (ref. 14) quantitative analysis of these errors is not complete.

8. CONCLUSIONS

The accuracy of the Forward Scattering Spectrometer Probe has been quantified and is shown to depend on many factors. The most important factor is the number density of the cloud. In clouds with a true number density of approximately 1000 per cm^3 centimeter the sizing error caused by coincidence events can be as high as 20 percent to 40 percent for the median volume diameter. Other factors, such as undersizing of large droplets and probe volume uncertainty, are also shown to be significant under certain conditions. Broadening of the size spectrum due to uneven laser beam illumination in the probe volume causes negligible errors in the measured average diameter and the median volume diameter.

Calibration devices for both the Forward Scattering Spectrometer Probe and the Optical Array Probe were developed and shown to be useful for both detailed calibration studies as well as field calibration. Also operation of the Forward Scattering Spectrometer Probe in an icing environment is discussed and recommendations were made to help alleviate some problems which may occur.

9. REFERENCES

1. Forward Scattering Spectrometer Probe: PMS Model FSSP-100, Operating and Servicing Manual. Particle Measuring Systems, Inc., Boulder, CO, 1984.
2. Dye, J.E.; and Baumgardner, D.: Evaluation of the Forward Scattering Spectrometer Probe. I: Electronic and Optical Studies. J. Atmos. Oceanic Technol., vol. 1, Dec. 1984, pp. 329-344.
3. Hovenac, E.A.: Calibration of Droplet Sizing and Liquid Water Content Instruments: Survey and Analysis. NASA CR-175099, 1986, pp. 16.
4. Baumgardner, D.; Strapp, W.; and Dye, J.E.: Evaluation of the Forward Scattering Spectrometer Probe. II: Corrections for Coincidence and Dead-Time Losses. J. Atmos. Oceanic Technol., vol. 2, Dec. 1985, pp. 626-632.
5. Cerni, T.A.: Determination of the Size and Concentration of Cloud Drops with an FSSP. J. Clim. Appl. Meteorol., vol. 22, Aug. 1983, pp. 1346-1355.
6. Pinnick, R.G.; Garvey, D.M.; and Duncan, L.D.: Calibration of Knollenberg FSSP Light-Scattering Counters for Measurement of Cloud Droplets. J Appl. Meteorol., vol. 20, Sept. 1981, pp. 1049-1057.
7. ASTM Standard: E799-81(1985): Standard Practice for Determining Data Criteria and Processing for Liquid Drop Size Analysis.
8. Young, B.W.; and Bachalo, W.D.: The Direct Comparison of Three In-Flight Droplet Sizing Techniques for Pesticide Spray Research. International Symposium on Optical Particle Sizing: Theory and Practice, Rouen, France, May 1987.
9. Norment, H.D.: Three-Dimensional Trajectory Analysis of Two Drop Sizing Instruments: PMS OAP and PMS FSSP. NASA CR-4113, 1988.
10. Hovenac, E.A.; Hirleman, E.D.; and Ide, R.F.: Calibration and Sample Volume Characterization of PMS Optical Array Probes. Presented at the 3rd International Conference on Liquid Atomization and Spray Systems (ICLASS 85), London, England. July 1985.
11. Hovenac, E.A.: Use of Rotating Reticles for Calibration of Single Particle Counters. LIA, vol. 58, 1987, pp. 129-134.
12. Hirleman, E.D.; Holve, D.J.; and Hovenac, E.A.: Calibration of Single Particle Sizing Velocimeters Using Photomask Reticles. ICLASS-Americas 2nd Annual Conference, Pittsburgh, PA, May 1988, pp. 38-41.
13. Reference Standards for Single Particle Counters, Insitec, 2110 Omega Road, San Ramon, CA 94583.
14. Baumgardner, D.: Corrections for the Response Times of Particle Measuring Probes. Sixth Symposium Meteorological Observations and Instrumentation, American Meteorological Society, Boston, MA, 1986, pp. 148-151.



Report Documentation Page

1. Report No. NASA CR-182293 DOT/FAA/CD-89/13	2. Government Accession No.	3. Recipient's Catalog No.
4. Title and Subtitle Droplet Sizing Instrumentation Used for Icing Research: Operation, Calibration, and Accuracy	5. Report Date August 1989	6. Performing Organization Code
	8. Performing Organization Report No. None (E-4538)	10. Work Unit No. 505-68-1A
7. Author(s) Edward A. Hovenac	11. Contract or Grant No. NAS3-25266	13. Type of Report and Period Covered Contractor Report Final
9. Performing Organization Name and Address Sverdrup Technology, Inc. NASA Lewis Research Center Group Cleveland, Ohio 44135	14. Sponsoring Agency Code	12. Sponsoring Agency Name and Address National Aeronautics and Space Administration Lewis Research Center Cleveland, Ohio 44135-3191 and Federal Aviation Administration, Technical Center Atlantic City International Airport, New Jersey 08405
15. Supplementary Notes Project Manager, Robert C. Anderson, Instrumentation and Control Division, NASA Lewis Research Center. FAA COTR, James T. Riley, Flight Safety Branch, Federal Aviation Agency.		
16. Abstract <p>The accuracy of the Forward Scattering Spectrometer Probe (FSSP) is determined using laboratory tests, wind tunnel comparisons, and computer simulations. Operation in an icing environment is discussed and a new calibration device for the FSSP (the rotating pinhole) is demonstrated to be a valuable tool. Operation of the Optical Array Probe is also presented along with a calibration device (the rotating reticle) which is suitable for performing detailed analysis of that instrument.</p>		
17. Key Words (Suggested by Author(s)) Calibration; Instrumentation; Laser applications; Aircraft icing; Droplet sizing; Cloud physics	18. Distribution Statement Unclassified-Unlimited Subject Category 35	
19. Security Classif. (of this report) Unclassified	20. Security Classif. (of this page) Unclassified	21. No of pages 54
		22. Price* A04

